

Preparation of carbon/carbon composite xerogels from resorcinol-formaldehyde and
cotton fiber for electric double layer capacitor



A Thesis Submitted in Partial Fulfillment of the Requirements
for the Degree of Master of Engineering in Chemical Engineering

Department of Chemical Engineering

Faculty of Engineering

Chulalongkorn University

Academic Year 2018

Copyright of Chulalongkorn University

การเตรียมซีโรเจลของคอมโพสิตคาร์บอน/คาร์บอน จากรีโซซินอล-ฟอร์มัลดีไฮด์ และเส้นใยฝ้าย
สำหรับตัวเก็บประจุไฟฟ้าสองชั้น



วิทยานิพนธ์นี้เป็นส่วนหนึ่งของการศึกษาตามหลักสูตรปริญญาวิศวกรรมศาสตรมหาบัณฑิต
สาขาวิชาวิศวกรรมเคมี ภาควิชาวิศวกรรมเคมี
คณะวิศวกรรมศาสตร์ จุฬาลงกรณ์มหาวิทยาลัย
ปีการศึกษา 2561
ลิขสิทธิ์ของจุฬาลงกรณ์มหาวิทยาลัย

กษะวัน ศิริจันทร์ : การเตรียมซีโรเจลของคอมโพสิตคาร์บอน/คาร์บอน จากรีโซซินอล-ฟอร์มาลดีไฮด์ และเส้นใยฝ้ายสำหรับตัวเก็บประจุไฟฟ้าสองชั้น. (Preparation of carbon/carbon composite xerogels from resorcinol-formaldehyde and cotton fiber for electric double layer capacitor) อ.ที่ปรึกษาหลัก : ผศ. ดร.พลัง บำรุงสกุลสวัสดิ์

งานวิจัยนี้สังเคราะห์ซีโรเจลของคอมโพสิตคาร์บอน/คาร์บอนเพื่อนำมาใช้เป็นขั้วอิเล็กโทรดสำหรับตัวเก็บประจุไฟฟ้าแบบสองชั้น เส้นใยฝ้ายถูกนำมาผสมกับพอลิเมอร์เจลซึ่งสังเคราะห์ผ่านปฏิกิริยาพอลิเมอร์ไรเซชันแบบควบแน่นระหว่างรีโซซินอลและฟอร์มาลดีไฮด์ ปฏิกิริยาถูกเร่งโดยโซเดียมคาร์บอเนตโดยน้ำกลั่นเป็นตัวทำละลาย เรโซซินอล-ฟอร์มาลดีไฮด์โซลถูกเทลงในขวดบรรจุที่มีเส้นใยฝ้าย หลังจากทิ้งไว้ให้เกิดเจลที่อุณหภูมิห้องและบ่มที่อุณหภูมิ 90 องศาเซลเซียสเป็นเวลาหนึ่งสัปดาห์ โมโนลิทที่เป็นรูพรุนที่เกิดขึ้นถูกหั่นเป็นแผ่นบาง จากนั้นนำแผ่นคอมโพสิตไปแช่ใน tert-butyl alcohol, ทำให้แห้งโดยรอบแห้งแบบสุญญากาศและดำเนินการไพโรไลซิสที่อุณหภูมิต่าง ๆ ภายใต้บรรยากาศไนโตรเจน ศึกษาผลของการใช้เส้นใยฝ้าย (0 - 40 เปอร์เซ็นต์โดยน้ำหนัก), อุณหภูมิในการไพโรไลซิส (600 - 1,000 องศาเซลเซียส) และเวลาในการกระตุ้นด้วยก๊าซคาร์บอนไดออกไซด์ (30, 60 และ 90 นาที) โครงสร้างจุลภาคและคุณสมบัติทางกายภาพได้ถูกวิเคราะห์โดยเทคนิคอินฟราเรดสเปกโตรสโกปี, เทคนิควิเคราะห์การเลี้ยวเบนของรังสีเอ็กซ์, การดูดซับหรือคายซับของก๊าซไนโตรเจน และกล้องจุลทรรศน์อิเล็กตรอนแบบส่องกราด ประสิทธิภาพทางเคมีไฟฟ้าของซีโรเจลของคอมโพสิตคาร์บอน/คาร์บอนได้รับการวิเคราะห์ในสารละลายโพแทสเซียมไฮดรอกไซด์ความเข้มข้น 4 โมลาร์ โดยใช้โพเทนชิโอมิเตอร์ในโหมดโวลแทมเมตรีและวัลคาไนซ์ประจุไฟฟ้า ซีโรเจลของคอมโพสิตคาร์บอน/คาร์บอนที่มีเส้นใยฝ้าย 10 เปอร์เซ็นต์โดยน้ำหนักและถูกกระตุ้นด้วยก๊าซคาร์บอนไดออกไซด์เป็นเวลา 90 นาที สามารถเก็บประจุได้มากที่สุด

สาขาวิชา วิศวกรรมเคมี
ปีการศึกษา 2561

ลายมือชื่อนิสิต
ลายมือชื่อ อ.ที่ปรึกษาหลัก

6070113421 : MAJOR CHEMICAL ENGINEERING

KEYWORD: Electric double-layer capacitor, Carbon xerogel, Composite, Cotton fiber

Kasawan Sirichan : Preparation of carbon/carbon composite xerogels from resorcinol-formaldehyde and cotton fiber for electric double layer capacitor. Advisor: Asst. Prof. Palang Bumroongsakulsawat, Ph.D.

This research used carbon/carbon composite xerogels as an electrode for EDLCs. Cotton fibers were blended with polymer gel which was synthesized through polycondensation between resorcinol and formaldehyde. The reaction was catalyzed by Na_2CO_3 with distilled water as a solvent. Resorcinol-formaldehyde sol was poured into a vial containing cotton fibers. After gelation at room temperature and curing at $90\text{ }^\circ\text{C}$ for a week, the resulting porous monolith was sliced into thin wafers. Then, the composite wafers were exchanged with tert-butyl alcohol, dried by vacuum drying and performed by pyrolysis at a various temperature under a nitrogen atmosphere, respectively. Effect of %cotton fibers loading (0-40 wt%), pyrolysis temperatures ($600 - 1000\text{ }^\circ\text{C}$) and CO_2 activation time (30, 60 and 90 min) were studied. The microstructure and the physical properties were characterized by Fourier transform infrared spectroscopy, X-ray diffraction, nitrogen adsorption-desorption, and scanning electron microscopy. The electrochemical performance of the carbon/carbon composite xerogels were analyzed in 4M potassium hydroxide aqueous solutions by potentiostat in cyclic voltammetry and galvanostatic charge-discharge mode. The activated carbon/carbon composite xerogels, which is 10 wt.% cotton fibers and CO_2 activation 90 min, have the highest specific capacitance.

Field of Study: Chemical Engineering

Student's Signature

Academic Year: 2018

Advisor's Signature

ACKNOWLEDGEMENTS

First of all, I would like to thank my thesis advisor, Asst. Prof. Palang Bumroongsakulsawat for his guidance, kindness advice and suggestions.

Furthermore, I would also like to thank my thesis committee members: Asst. Prof. Suphot Phatanasri, Asst. Prof. Pattaraporn Kim and Assoc. Prof. Kriangsak Kraiwattanawong for serving as my committee members and giving the comments and suggestions on early works and drafts of the research.

Last but not least, the author would like to thank all those who had helped directly or indirectly towards the completion of this thesis.

Finally, I would like to express my deepest gratitude and sincerest thank my family for always giving their countless love, encouragement, understanding and financial support throughout the study.

Kasawan Sirichan

TABLE OF CONTENTS

	Page
.....	iii
ABSTRACT (THAI).....	iii
.....	iv
ABSTRACT (ENGLISH).....	iv
ACKNOWLEDGEMENTS.....	v
TABLE OF CONTENTS.....	vi
LIST OF TABLES.....	x
LIST OF FIGURES.....	xi
CHAPTER 1 INTRODUCTION.....	1
1.1 Background.....	1
1.2 Research objectives.....	3
1.2.1 To synthesize the carbon/carbon composite xerogel from resorcinol– formaldehyde and cotton fibers.....	3
1.2.2 To study the effects of CO ₂ activation on carbon/carbon composite xerogel.....	3
1.2.3 To study the electrochemical performance of carbon/carbon composite xerogel as an electric double-layer capacitor (EDLC) electrode.....	3
1.3 Research scopes.....	3
1.3.1 The percent loading of cotton fibers (0 – 40%).....	3
1.3.2 The pyrolysis temperature with 600 – 1000 °C.....	3
1.3.3 The CO ₂ activation time (30 – 90 min) at 950 °C.....	3
CHAPTER 2 THEORY & LITERATURE REVIEW.....	4

2.1 Theory.....	4
2.1.1 Resorcinol-Formaldehyde gel (RF gel).....	4
2.1.2 Physical activation	6
2.1.3 Cotton fibers	6
2.1.4 Electric double-layer capacitor (EDLC).....	7
2.1.5 Electrolyte	7
2.1.5.1 Aqueous electrolyte	7
2.1.5.2 Organic electrolyte.....	7
2.1.6 Electrochemical cell design for performance testing.....	8
2.1.6.1 Three-electrode system.....	8
2.1.7 Electrochemical techniques	8
2.1.7.1 Cyclic voltammetry	8
2.1.7.2 Galvanostatic charge-discharge (GCD)	9
2.2 Literature review.....	10
2.2.1 Synthesis carbon xerogel	10
2.2.2 Pyrolysis Temperature	10
2.2.3 Carbon/carbon composite xerogel	11
2.2.4 CO ₂ activation of carbon xerogel.....	11
2.2.5 Carbon xerogel electrode for EDLC	12
CHAPTER 3 METHODOLOGY	13
3.1 Synthesis carbon/carbon composite xerogels	13
3.2 CO ₂ activation of carbon/carbon composite xerogels.....	14
3.3 Characterization.....	14
3.3.1 Scanning Electron Microscopy (SEM)	14

3.3.2 X-ray diffraction (XRD).....	15
3.3.3 Fourier Transform Infrared Spectroscopy (FT-IR).....	15
3.3.4 N ₂ adsorption/desorption isotherm analysis.....	15
3.4 Electrochemical measurements.....	15
CHAPTER 4 RESULTS AND DISCUSSIONS	17
4.1 Characterizations of carbon/carbon composite xerogels	17
4.1.1 Surface morphology.....	17
4.1.2 Phase analysis.....	21
4.1.3 Fourier transform infrared analysis.....	24
4.1.4 Surface area and porosity analysis.....	26
4.2 Electrochemical performances of carbon/carbon composite xerogels electrodes	34
4.2.1 Effect of % cotton fibers loading.....	34
4.2.2 Effect of various pyrolysis temperatures	39
4.2.3 Effect of CO ₂ activations.....	43
CHAPTER 5 CONCLUSIONS.....	49
5.1 Conclusions	49
5.2 Recommendations	50
REFERENCES	51
APPENDICES.....	55
Appendix A: Calculations for carbon/carbon composite xerogels and content of cotton fibers.....	55
Appendix B: Calculations for the specific capacitance	56
VITA.....	59



จุฬาลงกรณ์มหาวิทยาลัย
CHULALONGKORN UNIVERSITY

LIST OF TABLES

	Page
Table 4-1 Porous properties of the carbon/carbon composite xerogels obtained under different of cotton fibers at a carbonization temperature of 1000 °C.....	27
Table 4-2 Porous properties of the carbon/carbon composite xerogels obtained under different pyrolysis temperature at a content of 10 wt% cotton fibers.....	29
Table 4-3 Porous properties of the carbon/carbon composite xerogels obtained under different CO ₂ activation time at a content of 0 and 10 wt% cotton fibers	31
Table A-1 Synthesis conditions of carbon/carbon composite xerogels.....	52
Table A-2 The amount of precursors for carbon/carbon composite xerogels synthesis.....	52
Table A-3 The amount of cotton fibers for carbon/carbon composite xerogels synthesis.....	52

LIST OF FIGURES

	Page
Figure 2.1 Synthesis of the organic gel by the sol-gel methodology	4
Figure 2.2 Scheme of the addition reaction between resorcinol and formaldehyde... 5	5
Figure 2.3 Scheme of the condensation reaction between resorcinol and formaldehyde..... 5	5
Figure 2.4 Structure of cotton fiber	6
Figure 2.5 A schematic of charged EDLCs..... 7	7
Figure 2.6 Schematic drawing of a three-electrode system	8
Figure 2.7 Cyclic voltammogram curves of (a) ideal capacitor, (b) EDLC, and (c) pseudocapacitive materials..... 9	9
Figure 2.8 Galvanostatic charge-discharge plots of (a) EDLC and (b) pseudocapacitive material..... 9	9
Figure 4.1 SEM images of the internal structure of carbon/carbon composite xerogels : a) CC0_1000C, b) CC10_1000C, c) CC20_1000C, d) CC30_1000C and e) CC40_1000C	18
Figure 4.2 SEM images of the internal structure of carbon/carbon composite xerogels : a) CC0_600C, b) CC0_700C, c) CC0_800C, d) CC0_900C and e) CC0_1000C at magnification of 10,000x	19
Figure 4.3 SEM images of the internal structure of carbon/carbon composite xerogels : a) CC0_600C, b) CC0_700C, c) CC0_800C, d) CC0_900C and e) CC0_1000C at magnification of 40,000x	19
Figure 4.4 SEM images of the internal structure of carbon/carbon composite xerogels : a) CC10_600C, b) CC10_700C, c) CC10_800C, d) CC10_900C and e) CC10_1000C at magnification of 6,000x.....	20

Figure 4.5 SEM images of the internal structure of carbon/carbon composite xerogels : a) CC10AC0, b) CC10AC30, c) CC10AC60 and d) CC10AC90 at magnification of 6,000x	21
Figure 4.6 XRD patterns of the carbon/carbon composite xerogels obtained under different content of cotton fibers.	22
Figure 4.7 XRD patterns of the carbon/carbon composite xerogels obtained under different pyrolysis temperature.	22
Figure 4.8 XRD patterns of the carbon/carbon composite xerogels obtained under different CO ₂ activation time.	23
Figure 4.9 FTIR spectra of the carbon/carbon composite xerogels obtained under different content of cotton fibers.	24
Figure 4.10 FTIR spectra of the carbon/carbon composite xerogels obtained under different carbonization temperature.	25
Figure 4.11 FTIR spectra of the carbon/carbon composite xerogels obtained under different CO ₂ activation time.	26
Figure 4.12 Nitrogen adsorption-desorption isotherms of carbon/carbon composite xerogels obtained under a pyrolysis temperature of 1000 °C and different content of cotton fibers.	28
Figure 4.13 BJH pore size distribution for carbon/carbon composite xerogels obtained under different content of cotton fibers.	28
Figure 4.14 Nitrogen adsorption-desorption isotherms of carbon/carbon composite xerogels obtained under different pyrolysis temperature.	30
Figure 4.15 BJH pore size distribution for carbon/carbon composite xerogels obtained under different pyrolysis temperature.	30
Figure 4.16 Nitrogen adsorption-desorption isotherms of carbon/carbon composite xerogels obtained under different CO ₂ activation time.	32

Figure 4.17 BJH pore size distribution for activated carbon/carbon composite xerogels obtained under different CO ₂ activation time.....	32
Figure 4.18 Nitrogen adsorption-desorption isotherms of carbon/carbon composite xerogels obtained under a CO ₂ activation 90 min using with and without cotton fibers.....	33
Figure 4.19 BJH pore size distribution for activated carbon/carbon composite xerogels obtained under a CO ₂ activation 90 min using with and without cotton fibers.....	34
Figure 4.20 Cyclic voltammetry curves of the carbon/carbon composite xerogel electrodes at a scan rate of 0.3 mV s ⁻¹ in 4M KOH.....	35
Figure 4.21 specific capacitance from cyclic voltammograms of the carbon/carbon composite xerogel electrodes obtained under different content of cotton fibers. at a scan rate of 0.3 mV s ⁻¹ in 4M KOH.....	36
Figure 4.22 Cyclic voltammetry curves of CC10_1000C electrodes at different scan rates using in 4M KOH.....	36
Figure 4.23 Galvanostatic charge-discharge curves of the carbon/carbon composite xerogel electrodes at a current density of 0.5 A g ⁻¹ in 4M KOH.....	37
Figure 4.24 specific capacitance from discharge curves of the carbon/carbon composite xerogel electrodes obtained under different content of cotton fibers at a scan rate of 0.3 mV s ⁻¹ in 4M KOH.....	38
Figure 4.25 Galvanostatic charge-discharge curves of CC10_1000C electrodes at different current density using in 4M KOH.....	38
Figure 4.26 Cyclic voltammetry curves of the carbon/carbon composite xerogel electrodes obtained under different pyrolysis temperature at a scan rate of 0.3 mV s ⁻¹ in 4M KOH.....	40
Figure 4.27 Specific capacitance from cyclic voltammogram of carbon/carbon composite xerogels obtained under different pyrolysis temperatures.....	40

Figure 4.28 resistance value of carbon/carbon composite xerogels obtained under different pyrolysis temperatures	41
Figure 4.29 Galvanostatic charge-discharge curves of the carbon/carbon composite xerogel electrodes obtained under different pyrolysis temperature at a scan rate of 0.3 mV s^{-1} in 4M KOH.	42
Figure 4.30 Specific capacitance from discharge curves of carbon/carbon composite xerogels obtained under different pyrolysis temperatures	42
Figure 4.31 Cyclic voltammetry curves of the carbon/carbon composite xerogel electrodes obtained under different CO_2 activation time at a scan rate of 0.3 mV s^{-1} in 4M KOH.	44
Figure 4.32 Specific capacitance from cyclic voltammogram of carbon/carbon composite xerogels obtained under different CO_2 activation time	44
Figure 4.33 Cyclic voltammetry curves of CC10AC90 electrodes at different scan rates using in 4M KOH.....	45
Figure 4.34 Galvanostatic charge-discharge curves of the carbon/carbon composite xerogel electrodes obtained under different CO_2 activation time at a scan rate of 0.3 mV s^{-1} in 4M KOH.....	46
Figure 4.35 Specific capacitance from discharge curves of carbon/carbon composite xerogels obtained under different CO_2 activation time.....	47
Figure 4.36 Galvanostatic charge-discharge curves of CC10AC90 electrodes at different current density using in 4M KOH	47

CHAPTER 1

INTRODUCTION

1.1 Background

At present, global warming and the shortage of oil from fossils causing society to focus on sustainable alternative energy such as solar energy and wind energy. They are gaining much attention. In order to use those alternative energies, it is necessary to have efficient energy storage. Electric double layer capacitors (EDLCs), a type of electrochemical capacitors, are promising the energy storage device owing to their high power density, the reversibility and the long cycle life[1]. However, EDLCs also have a low energy density compared with a Lithium-ion battery. Electrode materials are one of the most important factors for the improvement of the electrochemical performance of EDLCs. Carbon materials are used as the electrode for EDLCs due to their high surface area[2].

Carbon gels are interesting in the field of carbon materials after it was firstly reported by Pekala in 1989[3]. Carbon gels are prepared via a sol-gel process involving resorcinol (R) and formaldehyde (F) as a carbon precursor. The most important properties of carbon gel materials, like carbon aerogel, cryogel and xerogel based on resorcinol (R) and formaldehyde (F) are: the surface area, the pore volume, the controllable pore structure and the low electrical resistivity. Most of the previous works focused on carbon aerogels and cryogels because of the carbon xerogels are the high pore shrinkage during the drying process. Nevertheless, the carbon xerogels are more cost effective since the convenient drying method and the inexpensive equipment. The carbon composite cryogels with cotton fibers can improve the specific capacitance of electrodes for EDLCs[4]. The preparation of carbon/carbon composites can decrease the production cost by using inexpensive and renewable cotton fibers as a starting material[5]. In literature reports the pyrolysis temperature used to prepare carbon xerogels was in the range of 600 – 1050 °C [6, 7]. The

pyrolysis process more challenging to prepare the carbon xerogels. Therefore, the low pyrolysis temperature can decrease the production cost on an industrial scale to make carbon xerogels[8].

In order to enhance the quality of the carbons, the porous carbons were usually treated by pyrolyzing the waste materials with physical additives as agents for further activation. CO₂ activation is one of the most common techniques used to increase the microporosity of carbon materials[9-11]. By varying the activation conditions, it should be possible to control the micropore development of carbon gels within an already controlled mesopore and macropore network[12]. The CO₂ activation method has the several advantages without the corrosive agent, contributing to the activated carbon materials with the very low ash content and these activated carbon materials do not require a washing posttreatment[13]. In this work, the carbon/carbon composite xerogels from RF gels and cotton fibers are synthesized. In addition, the effect of different loading cotton fibers, the pyrolysis temperature and the CO₂ activation time on the porous properties and the electrochemical performances of carbon/carbon composite xerogels are studied.

1.2 Research objectives

1.2.1 To synthesize the carbon/carbon composite xerogel from resorcinol-formaldehyde and cotton fibers.

1.2.2 To study the effects of CO₂ activation on carbon/carbon composite xerogel.

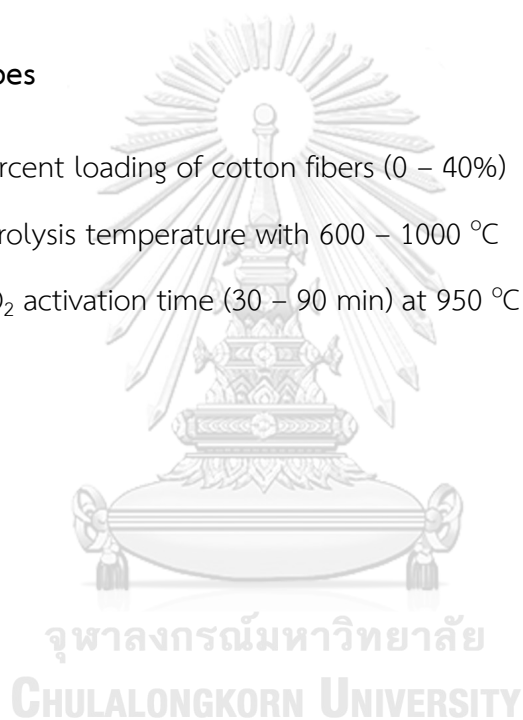
1.2.3 To study the electrochemical performance of carbon/carbon composite xerogel as an electric double-layer capacitor (EDLC) electrode.

1.3 Research scopes

1.3.1 The percent loading of cotton fibers (0 – 40%)

1.3.2 The pyrolysis temperature with 600 – 1000 °C

1.3.3 The CO₂ activation time (30 – 90 min) at 950 °C



CHAPTER 2

THEORY & LITERATURE REVIEW

2.1 Theory

2.1.1 Resorcinol-Formaldehyde gel (RF gel)

The first patented carbon gel was reported by Pekala[3]. They synthesized the low density of organic aerogels from resorcinol and formaldehyde, which are the precursors of carbon gels[14]. The polymerization reaction occurs between resorcinol and formaldehyde, which a liquid gradually condenses from a stable suspension of colloidal solid particles (sol) to create a three-dimensional porous network in a liquid medium (gel)[15], as shown in Figure 2.1.

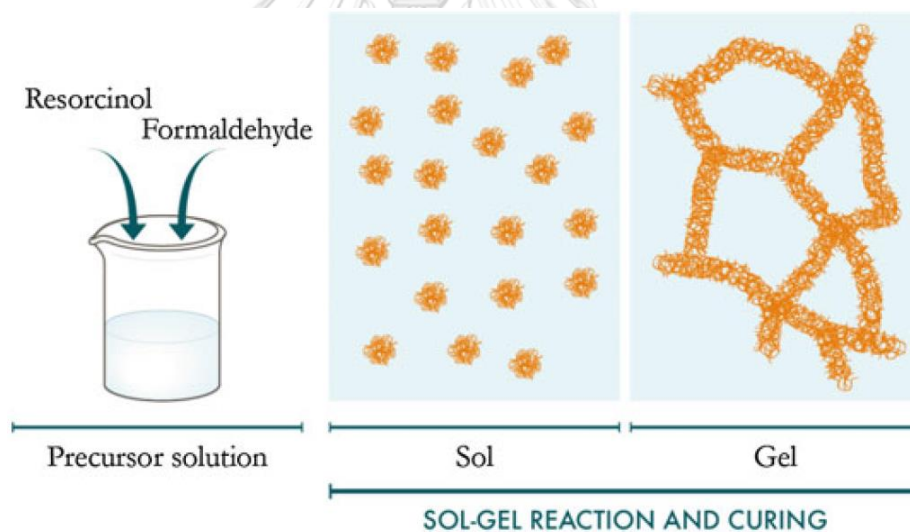


Figure 2.1 Synthesis of the organic gel by the sol-gel methodology[15]

The polymerization reaction involves two main stages: (1) an addition reaction, as shown in Figure 2.2 and (2) a condensation reaction, as shown in Figure 2.3. Resorcinol is a trifunctional benzyl compound with two hydroxyl groups at position 1 and 3 which allows formaldehyde to be added in positions 2, 4 and 6 [14]. At the same time, a condensation occurs. The hydroxymethyl derivatives lose OH- groups

from benzyl-type cations and react with other benzene rings, giving methylene and ether bonds[3]. Polymer particles are then formed.

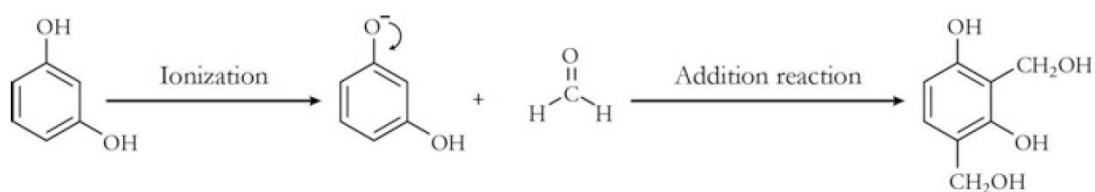


Figure 2.2 Scheme of the addition reaction between resorcinol and formaldehyde

[15]

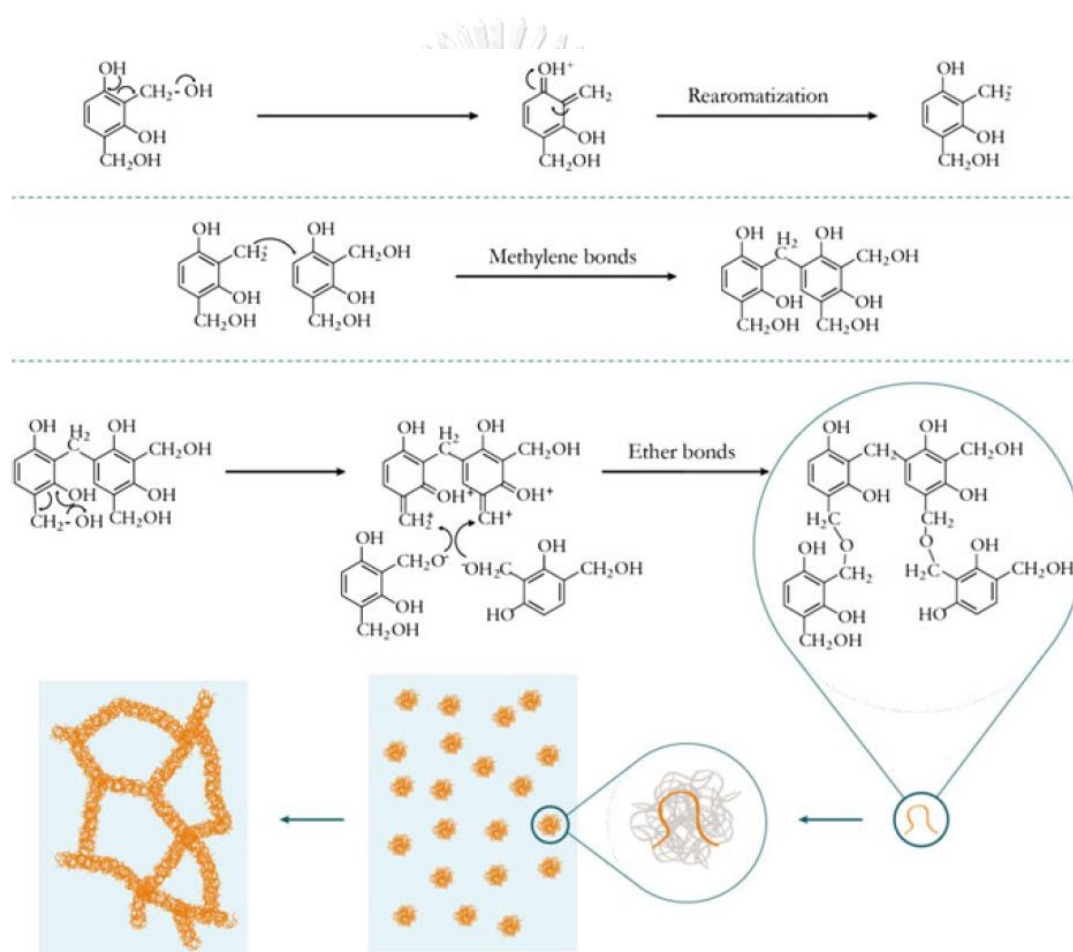


Figure 2.3 Scheme of the condensation reaction between resorcinol and formaldehyde[15]

2.1.2 Physical activation

The RF xerogels can be activated during or after pyrolysis with gases[16]. CO₂ and steam are two activating gases used in the physical activation of carbons. Activating gases react with the carbon structures to produce CO, CO₂, H₂ or CH₄. The degree of activation is normally referred to as “burn-off” and it is defined as the weight difference between the carbon and the activated carbon divided by the weight of the original carbon on dry basis according to with the following equation,

$$\%Burn\ off = \frac{W_0 - W_1}{W_0} \times 100$$

Where W₀ is the weight of the original carbon and W₁ refers to the mass of the activated carbon. The use of CO₂ during the activation process of a carbon material develops narrow micropores, while steam widens the initial micropores of the carbon[11]. Physical activation methods have advantages in that they do not require any corrosive agents, leading to activated carbons with very low ash content and not requiring a washing posttreatment[10].

2.1.3 Cotton fibers

Cotton is the dominant natural fibers that purest form of cellulose available in nature. Under the microscope, it looks like a twisted ribbon. Cotton has a multilayered structure which consists of a primary wall, a secondary wall and lumen, as shown in Figure 2.4. Cotton fiber consists of cellulose (90%) waxes, protein, pectate and minerals[17].

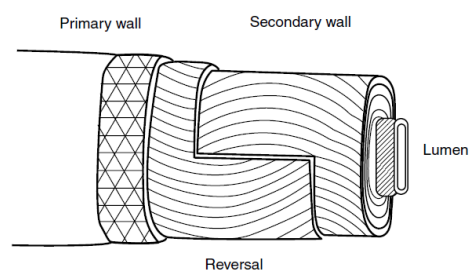


Figure 2.4 Structure of cotton fiber[17]

2.1.4 Electric double-layer capacitor (EDLC)

EDLCs have a similar mechanism with conventional capacitors. The charges are stored on the interfaces between the electrode and the electrolytes for their energy storage. A potential difference across the electrodes leads to a migration of electrolyte ions to the pores of electrodes[18]. , as shown in Figure 2.5.

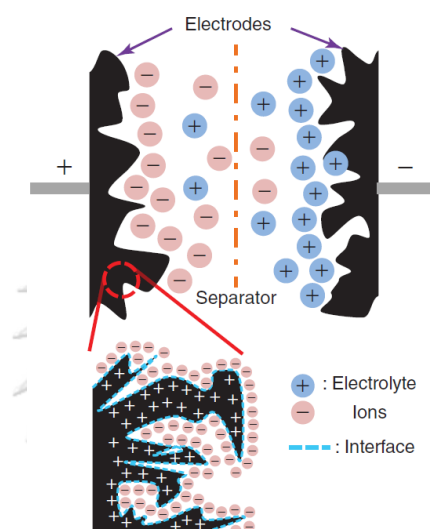


Figure 2.5 A schematic of charged EDLCs [18]

2.1.5 Electrolyte

2.1.5.1 Aqueous electrolyte

Aqueous electrolytes are primarily adopted in research stages for their low cost and abundance. KOH is the common aqueous electrolytes bearing the merits of easy handling in an open environment and low ionic resistivity[18].

2.1.5.2 Organic electrolyte

Most of the commercial supercapacitors used organics electrolytes such as propylene carbonate (PC) and acetonitrile because of their wide operating voltage windows (0 to 2.2-2.7). The board voltage range raises the energy density to the standard of commercial demand[18].

2.1.6 Electrochemical cell design for performance testing

2.1.6.1 Three-electrode system

The three-electrode system consists of a working electrode, a reference electrode, and a counter electrode, which are all connected to a potentiostat. This potentiostat is used to control the electrode potential while recording the change in electrode current with potential, or controlling the current passing through the electrode and then recording the change in electrode potential with current[18]. The three operating components: (a) working electrode, (b) reference electrode, and (c) counter electrode, as shown in Figure 2.6.

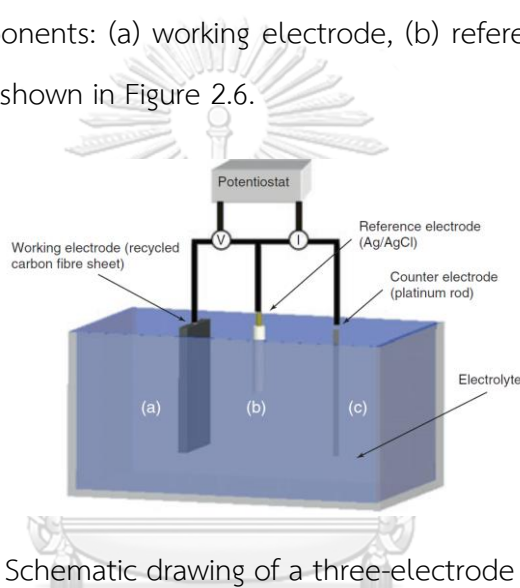


Figure 2.6 Schematic drawing of a three-electrode system [19]

2.1.7 Electrochemical techniques

2.1.7.1 Cyclic voltammetry

This technique applies a potential to the working electrode, concerning the reference electrode's fixed potential, which linearly sweeps back and forth between the two predefined potentials. Cyclic voltammetry assesses quantitative and qualitative data relating to the electrochemical phenomena occurring in the active materials of the working electrode. The potential range is limited by electrolyte's operating stability[18]. Scanning the potential range yields a time-dependent current and plotting this current (I) against the scanned potential (E) graphs a cyclic voltammogram (CV) curve for capacitance diagnosis.

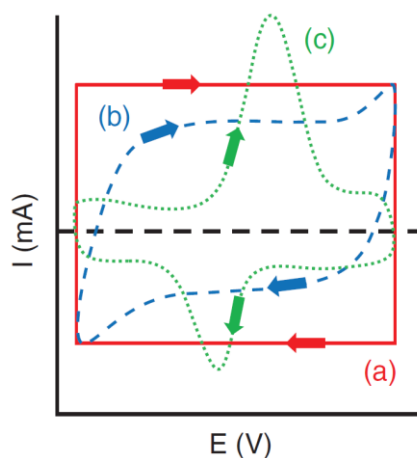


Figure 2.7 Cyclic voltammogram curves of (a) ideal capacitor, (b) EDLC, and (c) pseudocapacitive materials.

2.1.7.2 Galvanostatic charge-discharge (GCD)

GCD is an alternative method to measure the capacitance of the material. The GCD technique applies a constant current density (e.g., A/g) and measures the responsive potential concerning time. Generally, the working electrode is charged to a preset potential and the discharge process is then monitored to assess the capacitance[18].

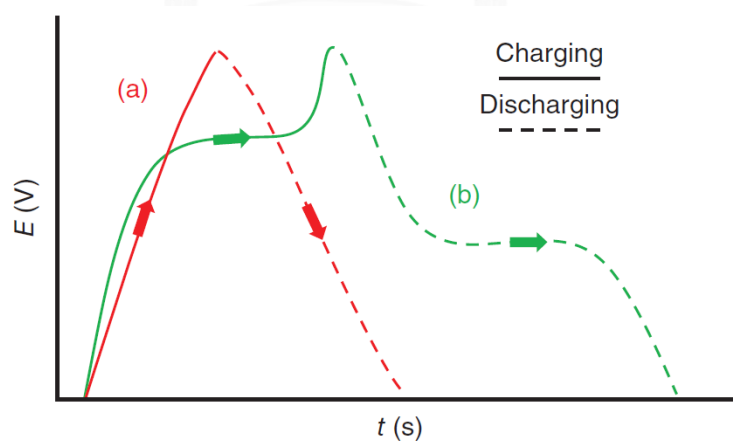


Figure 2.8 Galvanostatic charge-discharge plots of (a) EDLC and (b) pseudocapacitive material

2.2 Literature review

2.2.1 Synthesis carbon xerogel

Carbon gels can be obtained following the different procedures[16] but the preparation mainly consists of three steps: (i) the gel synthesis, involving the formation of a three-dimensional polymer in a solvent (gelation), followed by a curing period, (ii) gel drying, where the solvent is removed to obtain an organic gel, and (iii) pyrolysis under an inert atmosphere to form the porous carbon material, i.e. the so-called carbon gel. Among others, resorcinol-formaldehyde (RF) aqueous gels are the most studied systems[12, 15].

2.2.2 Pyrolysis Temperature

Pyrolysis is a thermochemical decomposition of organic materials at elevated temperatures in argon or nitrogen atmosphere[20]. Pyrolysis of carbon gels are generally operated within the temperature range from 500 to 900 °C for 0.5 to 3 hours[13]. The microporosity is mostly developed during the pyrolysis conditions. Under the pyrolysis step, the physical property particularly undergoes modifications and it depends on the texture of starting materials[13, 15].

Lin C. et al. [20] studied the evolution of the pore structure of carbon xerogels derived from resorcinol-formaldehyde resins with an increase of carbonization temperature. The RF mole ratio was fixed at 0.5. The gel was solvent exchange with acetone. The carbon xerogels were carbonized at 600 to 1200 °C for 3 h in N₂. They reported that the loss of microporosity when carbonization temperature was increased. In the mesopore changed insignificantly with the carbonization temperature. The surface area decreased from 850 to 600 m² g⁻¹ when the carbonization temperature increased from 600 to 1200 °C.

Moreno A.H. [8] synthesized organic xerogels from the microwave-assisted synthesis of resorcinol and formaldehyde by the sol-gel method. The organics

xerogel was carbonized from room temperature to three different final temperatures (750, 850 and 950 °C) at heating rate 5 °C min⁻¹. Researcher founded that properties before and after pyrolysis is due to the loss of heteroatoms (i.e., oxygen, hydrogen) in the polymer network being released as CO₂ and CH₄ or other organic molecules during pyrolysis[21]. They observed that the increase of carbonization temperature causes a decrease in porosity.

2.2.3 Carbon/carbon composite xerogel

Kraiwattanawong K. et al. [5] prepared a carbon/carbon composite cryogel from the cotton fiber dispersed in the RF gel matrix. Cotton fibers to RF mass ratio was 0, 0.05, 0.10, 0.15, 0.20 and 0.25 g/g. The carbon/carbon composite cryogels were pyrolyzed at 1000 °C. Cotton fibers would be converted to carbon fibers by pyrolysis. They reported that composite has the nanoporous carbon spheres with the surrounding nanocages and the carbon fiber. They founded that the preparation of C/C composites cannot have an influence on the micropores.

2.2.4 CO₂ activation of carbon xerogel

The CO₂ activation is a physical activation of the carbonized sample carried out at 800 to 950 °C for the removal of the contaminants. When CO₂ activation was applied, the activated carbon gels are produced with the high micropore volume and the high mesopore volume[9].

Lin C. et al. [20] studied the evolution of the pore structure of carbon xerogels derived from the resorcinol-formaldehyde resins with an increase of carbonization temperature and the CO₂ activation times. The RF mole ratio was fixed at 0.5. The gel was solvent exchange with acetone. The carbon xerogels were carbonization at 1050 °C from 3 h in nitrogen. For the activation, N₂ containing 5 vol% CO₂ for 0 - 3 h. The creation and the destruction of small micropores in the 0.6 nm range were increased by the CO₂ activation time. They founded that the total surface area

increased from 600 to 1600 m² g⁻¹ with an increase in the CO₂ activation time from 0 to 3 h.

Mari'a et al. [10] synthesized carbon xerogels from resorcinol-formaldehyde as a carbon precursor. They studied the effect of physical activation with CO₂ and the chemical activation with KOH. The carbon xerogels were pyrolyzed at 900 °C. Researchers reported that these processes increase the micropore volume and specific surface area. The specific surface area increases from 600 m² g⁻¹ to 2000 m² g⁻¹ increasing the temperature and the duration of an activation step.

2.2.5 Carbon xerogel electrode for EDLC

Kraiwattanawong K. et al. [4] prepared a carbon/carbon (C/C) composite cryogel used as the EDLC electrode. The molar ratio of resorcinol to formaldehyde were fixed at 0.5 mol/mol. The carbon/carbon composites had the carbon tunnel structure in any content of cotton fibers. The sample was used as the electrode under a 3-cell electrode analysis. In the 4M KOH solution. They reported that the capacitance could be increased with the increase of the content of cotton fibers added to the C/C composites.

Takanori et al. [22] prepared the high surface area carbon xerogels in the disks form by the activation with CO₂ at 1000 °C. The RF gels prepared at R/C ratios of 50, 200, and 1000. They founded that BET surface increased when the activation time was increased, and ultimately reached a high surface area of 3000 m²g⁻¹ at a burn-off of 79%. The carbon xerogels disks shape were used as an electrode for an EDLC without a binder. Electrochemical performances using two electrode cells. A 30 wt.% H₂SO₄ solution was used as the electrolyte solution. It gave the highest specific capacitance 251 F g⁻¹ at scan rate 2 mV s⁻¹.

CHAPTER 3

METHODOLOGY

3.1 Synthesis carbon/carbon composite xerogels

The carbon/carbon composite xerogel was synthesized by pouring the RF sol into a vial containing cotton fibers (0-40%). After the gelation at room temperature and curing at 90 °C for a week, the samples was sliced into thin wafers. Then, the composite wafers were exchanged with tert-butyl alcohol (TBA), dried by the vacuum drying and carbonized under nitrogen atmosphere, respectively. The RF sol was prepared by blending resorcinol (Sigma-Aldrich Chemistry, research grade, 99 wt.%), formaldehyde (Labsan Asia Co., Ltd, research grade, 35-40 wt.% stabilized by 4-12 wt.% methanol), sodium carbonate (Na_2CO_3) (Sigma-Aldrich Chemistry, research grade, 99.8%) as a basic catalyst and distilled water (W) as a solvent. The mass concentration of resorcinol to distilled water, the molar ratio of resorcinol to sodium carbonate, and the molar ratio of resorcinol to formaldehyde were fixed at 0.250 g/cm³, 200 mol/mol, and 0.5 mol/mol, respectively.

The RF sol was poured into 10 cm³ vials (ca. 16 mm inner diameter) containing the cotton fibers 0.0, 0.1, 0.2, 0.3 and 0.4 g/g (cotton/RF gels). Distilled water was used as diluents. The mixture was gelated at 25 °C to form a composite hydrogel. Subsequently, the composite hydrogels were cured by the conventional procedure at room temperature for 1 day, 50 °C for 1 day and 90 °C for a week, respectively. The composite hydrogels were sliced to be thin wafers (ca.1 mm thickness). Water in the composite hydrogel is exchanged with TBA before vacuum drying. The composite hydrogels were immersed in TBA for 4 days at 50 °C. Fresh TBA was exchanged once a day. The exchanged composite hydrogels were evacuated to obtain the RF composite xerogels. The carbon/carbon composites were prepared by pyrolyzing the RF composite xerogels in a quartz reactor placed inside a horizontal furnace. Nitrogen flowed through the quartz reactor at 200 cm³ min⁻¹. The

temperature was raised from room temperature to 250 °C at 250 °C hr⁻¹, and it was held at 250 °C for 2 h. Next, the temperature was ramped to the five different final temperatures (600, 700, 800, 900 and 1,000 °C) at 250 °C hr⁻¹, and it was held at final temperatures for 4 h. The cotton fibers are converted to the carbon fibers by the pyrolysis. The prepared carbon/carbon composite xerogel samples were denoted as CCX_YC where X represents % of cotton fibers and Y represents pyrolysis temperature.

3.2 CO₂ activation of carbon/carbon composite xerogels

The carbon/carbon composite xerogels pyrolyzed at 1,000 °C was activated with CO₂ gas. CO₂ activation of the carbon/carbon composite xerogels were performed by heating them in a 170 cm³ min⁻¹ N₂ flow of 15 vol% CO₂ in N₂ at 950 °C for 30, 60 and 90 min. After the CO₂ activation step, pure N₂ may be passed through the sample for 3 hours to replace CO₂ and cool down to room temperature. The activated carbon/carbon xerogels experienced some shrinkage but they retained their original thin wafer shape. The prepared CO₂ activated carbon/carbon composite xerogel samples were denoted as CCX_YAC where X represents % of cotton fibers and Y represents CO₂ activation time.

3.3 Characterization

3.3.1 Scanning Electron Microscopy (SEM)

The morphologies of carbon/carbon composite xerogels were studied using a scanning electron microscope (Hitachi S-3400N, Japan). The sample was coated with platinum (Pt) by sputtering coating device. Then the images of the sample were taken with magnification from 6,000 to 40,000 times.

3.3.2 X-ray diffraction (XRD)

The phase structure of each sample was analyzed by X-ray diffraction (XRD) using an X-ray diffractometer with $\text{CuK}\alpha$ radiation at a 2Θ range between $10\text{--}80^\circ$.

3.3.3 Fourier Transform Infrared Spectroscopy (FT-IR)

The Fourier-transform infrared was used to investigate the surface functional groups of carbon/carbon composite xerogel samples. FTIR spectra of carbon/carbon composite xerogel samples were recorded by using Nicolet 6700 FT-IR (Thermo Scientific, USA) in the wavenumber range $4,000\text{--}400\text{ cm}^{-1}$.

3.3.4 N_2 adsorption/desorption isotherm analysis

The porous properties, including the surface area, the pore volume and the pore diameter of these carbon/carbon composite xerogels were evaluated by N_2 adsorption/desorption isotherm analysis using BELSORP-mini II (BEL Japan) analyzer at $-196\text{ }^\circ\text{C}$. Before analysis, the carbon/carbon composite xerogel samples were degassed for 3 h at $180\text{ }^\circ\text{C}$ to remove all of the physisorbed species. The Brunauer-Emmett-Teller (BET) surface area was calculated by BET analysis. Micropore volume (V_{mic}) was analyzed by DA analysis. Mesopore volume (V_{mes}) and mesopore size distributions were analyzed by BJH (Barrett-Joyner-Halenda) analysis.

3.4 Electrochemical measurements

The electrochemical measurements were conducted using a three electrodes cell in 4M KOH aqueous electrolyte (Wako Pure Chemical Industries Inc., research grade, 8M). The carbon/carbon composite xerogels that are in the form of the thin wafer were used as working electrodes. Ag/AgCl (saturated KCl-filled) electrodes and Au wire were performed as a reference electrode and a counter electrode, respectively. Before the measurement, the carbon/carbon composite xerogels were soaked in the electrolyte solution under vacuum overnight. Electrochemical

performing was measured at room temperature. Cyclic voltammetry (CV) and galvanostatic charge-discharge (GCD) were performed using a AUTOLAB PGSTAT 101 potentiostat (Metrohm) running NOVA (version 2.1.4) software. The cyclic voltammetry was analyzed at a potential window range of -1 to 0 V (vs Ag/AgCl) with the scan rate of 3 – 500 mV s⁻¹. The galvanostatic charge/ discharge method is typically used at the current density of 0.5 – 2 A g⁻¹. The specific capacitance was calculated from the cyclic voltammogram (C_c) and the discharged curve (C_D) using Eqs. (1) and (2), respectively[5].

$$C_c = \frac{Q}{(\Delta V_c \times m \times \mu)} \quad (1)$$

$$C_D = \frac{I \Delta t}{(\Delta V_D \times m)} \quad (2)$$

where Q (charge) is derived from the half integrated area of the CV curve, ΔV_c is the potential window and μ is the scan rate of the C_v measurement. From the C_D study, the constant discharge current (I), discharge time (Δt) and discharge voltage (ΔV_D) were used to calculate the specific capacitance.

CHAPTER 4

RESULTS AND DISCUSSIONS

The results of the experiments are shown in this chapter. Characterizations of the carbon/carbon composite xerogels prepared from resorcinol-formaldehyde and cotton fibers. The effect of cotton fiber loading, carbonization temperature, and CO₂ activation time on pore structures, porous properties, and electrochemical performances of carbon/carbon composite xerogels are explained.

4.1 Characterizations of carbon/carbon composite xerogels

Resorcinol-formaldehyde gels (RF gels) blended with cotton fibers were conducted by pyrolysis in a nitrogen atmosphere to obtain carbon/carbon composite xerogels. The microstructure and the physical properties were characterized by scanning electron microscopy, x-ray diffraction, Fourier transform infrared spectroscopy and nitrogen adsorption-desorption.

4.1.1 Surface morphology

Scanning electron microscopy (SEM) was used to study the surface morphology of the carbon/carbon composites xerogels.

Effect of %loading cotton fiber on the morphology of the prepared carbon/carbon composite xerogels shows in SEM images (Figure 4.1). The SEM images show that all the carbon/carbon composite xerogels were formed a monolithic 3D mesoporous network of small carbon particles and hierarchical porous with micropores and mesopores of carbon/carbon composite xerogels[23-25]. From Figure 4.1 (b-e), the loading of cotton fibers conditions reveals carbon fiber and tunnel pore[5].

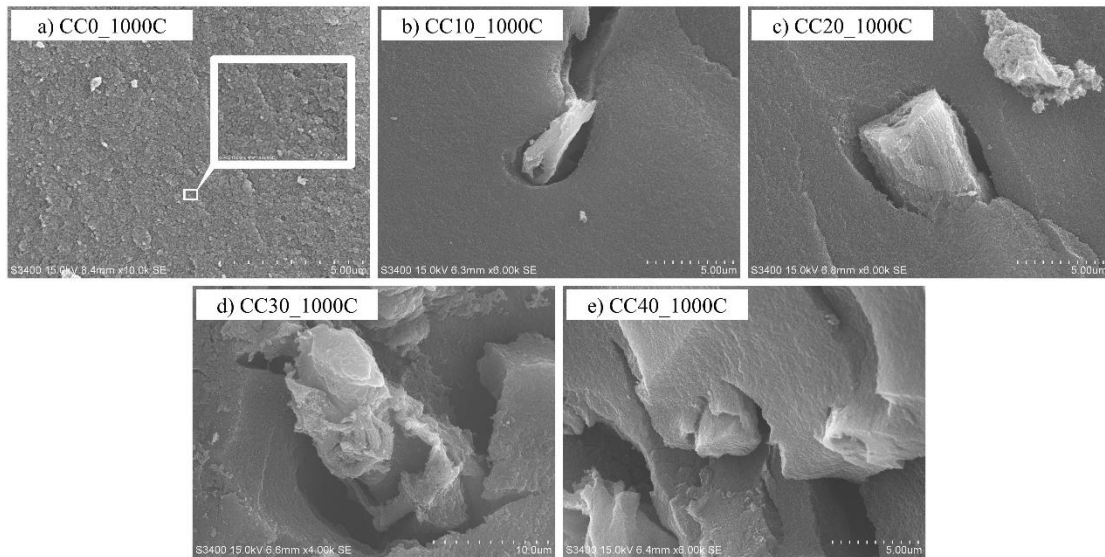


Figure 4.1 SEM images of the internal structure of carbon/carbon composite xerogels : a) CC0_1000C, b) CC10_1000C, c) CC20_1000C, d) CC30_1000C and e) CC40_1000C

Effect of pyrolysis temperature on the morphology of the prepared carbon/carbon composite xerogels shows in SEM images (Figure 4.2 – 4.3). The SEM images a three-dimensional interconnected network of small carbon particles[26]. The pore shapes are irregular. The small carbon particles start coming closer as the pyrolysis temperature increased. It is also found that more macropores randomly spread in the samples heated at 600 °C to 800 °C. It is likely that some colloids in xerogel structure decompose into volatile gases, due to the decomposition of resorcinol-formaldehyde and cotton fibers into carbon char. Moreover, large pores of carbon/carbon composite xerogels were pyrolyzed at 900 °C and 1000 °C are reduced because the larger volume shrinkage occurs at higher temperature[27].

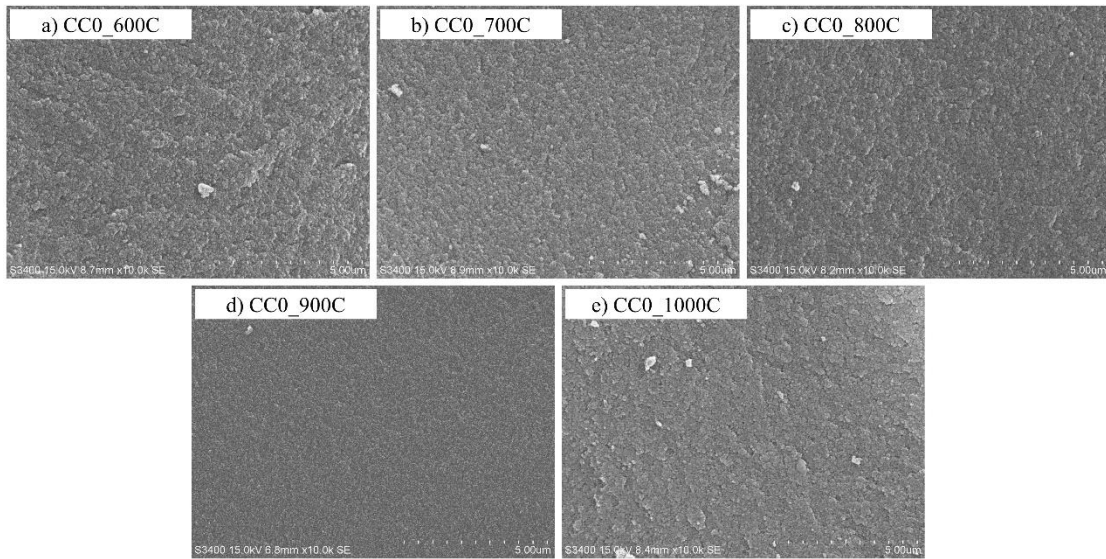


Figure 4.2 SEM images of the internal structure of carbon/carbon composite xerogels : a) CC0_600C, b) CC0_700C, c) CC0_800C, d) CC0_900C and e) CC0_1000C at magnification of 10,000x

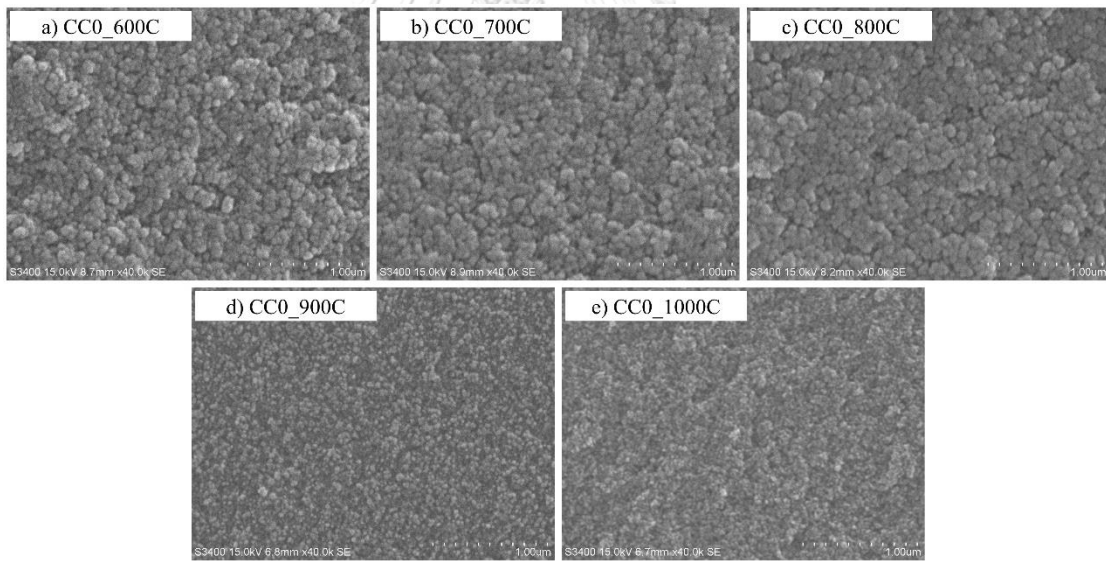


Figure 4.3 SEM images of the internal structure of carbon/carbon composite xerogels : a) CC0_600C, b) CC0_700C, c) CC0_800C, d) CC0_900C and e) CC0_1000C at magnification of 40,000x

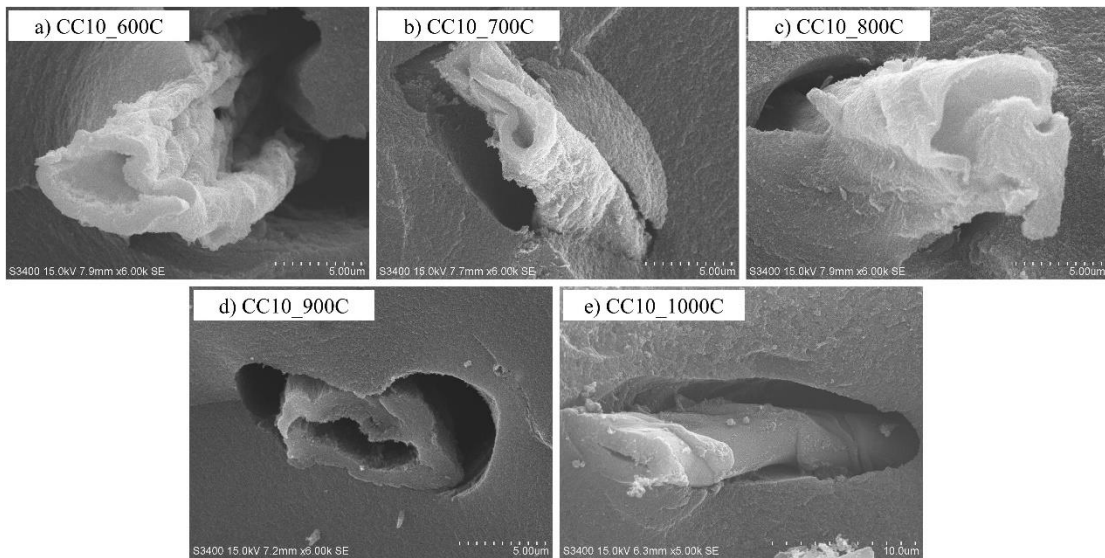


Figure 4.4 SEM images of the internal structure of carbon/carbon composite xerogels : a) CC10_600C, b) CC10_700C, c) CC10_800C, d) CC10_900C and e) CC10_1000C at magnification of 6,000x

Effect of CO_2 activation time on the morphology of the prepared carbon/carbon composite xerogels shows in SEM images. Figure 4.5 shows the SEM images of carbon/carbon composite xerogels before and after CO_2 activation. For CO_2 activation process under CO_2 gas in the range of activation time between 30 min to 90 min, and the activation temperature is fixed at 950 °C. They confirm that the 3D interconnected micropore and mesopore in carbon/carbon composite structure can be maintained in these activated carbon/carbon composite xerogels. Compared to the small carbon particles and porous morphology of CC10_1000C, a slightly loose and porous structure was observed in CC10AC90 [28].

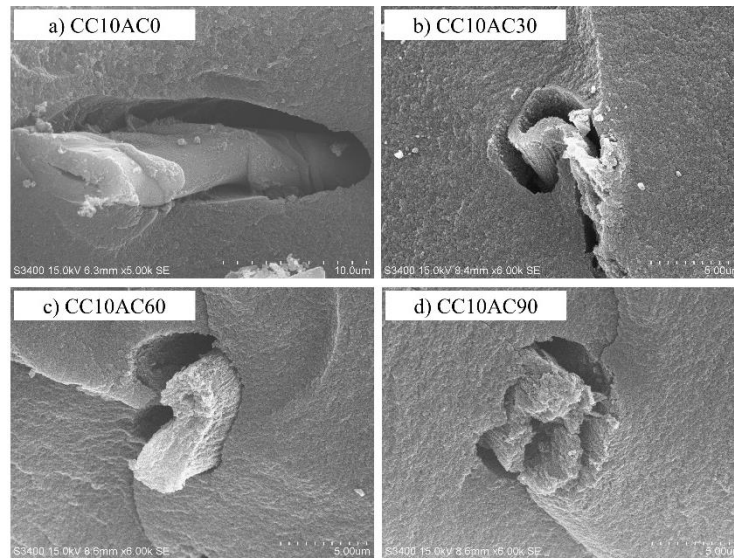


Figure 4.5 SEM images of the internal structure of carbon/carbon composite xerogels : a) CC10AC0, b) CC10AC30, c) CC10AC60 and d) CC10AC90 at magnification of 6,000x

4.1.2 Phase analysis

Figure 4.6 – 4.8 shows the XRD patterns of the carbon/carbon xerogels samples that were found to be almost identical but displayed two broad diffraction peaks, centered at around $2\theta = 23.5^\circ$ and 43.8° [29]. It can be observed that two broad reflections were found for all samples. Reflection of the hexagonal graphite peak (002) plane was ascribed to graphitic carbon, whereas the weaker diffraction peak was attributed to the rhombohedral graphite peak (101) crystal planes. These results demonstrate that the carbon/carbon composite xerogels are composed of partly graphitized carbon and partly graphite-like carbon[24] [30].

Figure 4.6 shows the XRD patterns of the carbon/carbon composite xerogels obtained under different wt.% cotton fibers loading. It is clear that all of the peaks have the same a wide and intensities. This indicates that loading cotton fiber does not change the phase structure of carbon/carbon composite xerogels.

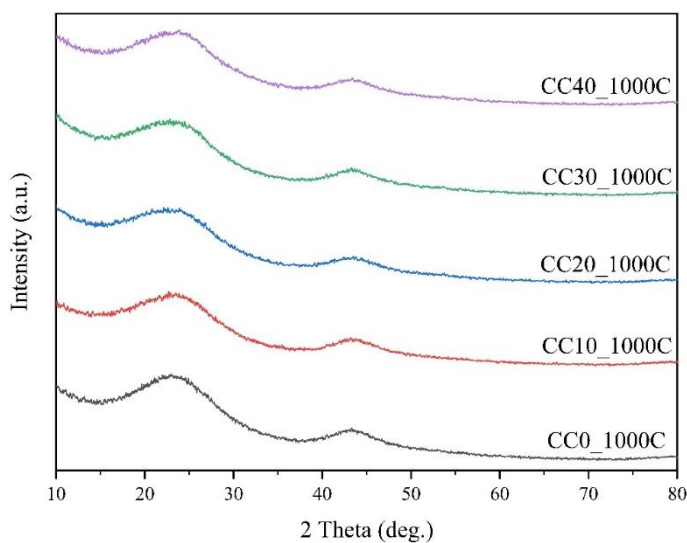


Figure 4.6 XRD patterns of the carbon/carbon composite xerogels obtained under different content of cotton fibers.

Figure 4.7 demonstrates the XRD patterns of carbon/carbon composite xerogels prepared at 600 °C, 700 °C, 800 °C, 900 °C and 1000 °C, respectively. The broad diffraction peaks are observed at $2\theta = 23.5^\circ$ and 43.8° in all samples. The peak at 43.8° also becomes high intensity as the pyrolysis temperature increased. This indicates that the carbon/carbon composite xerogels have more graphite region after increasing the pyrolysis temperature from 600 to 1000 °C.

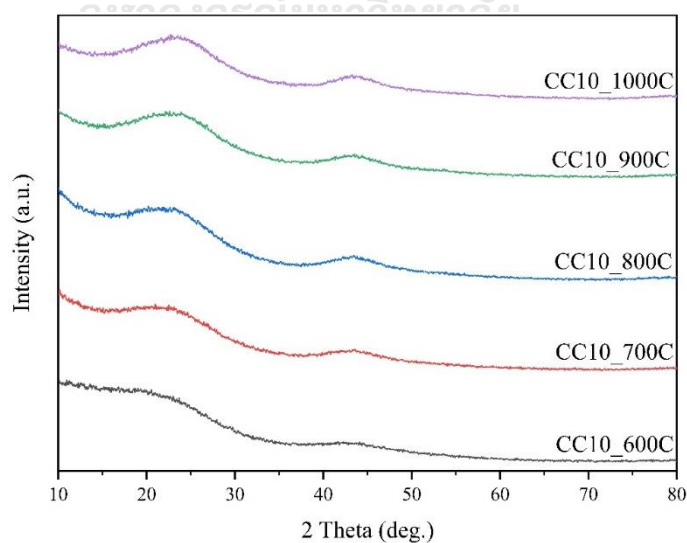


Figure 4.7 XRD patterns of the carbon/carbon composite xerogels obtained under different pyrolysis temperature.

Figure 4.8 illustrates the XRD patterns of carbon/carbon composite xerogels compares to the activated carbon/carbon composite xerogels at CO₂ activation time between 30 min to 90 min. All of the samples exhibit a broad peak at $2\theta = 23.5^\circ$ and 43.8° . Furthermore, it is clear that the diffraction peaks at $2\theta = 23.5^\circ$ become wide and their intensities decreased as CO₂ activation time increased, especially for the (002) diffraction peak. The results show that CO₂ etching reduces the order of the carbon/carbon composite xerogels structure due to the formation of micropores or defects[31]. This indicates that the CO₂ activation times are affected by the structure of the activated carbon/carbon composite xerogels. In addition, several publications suggest that graphite can be reconstructed into the carbon in randomly oriented layers [32, 33].

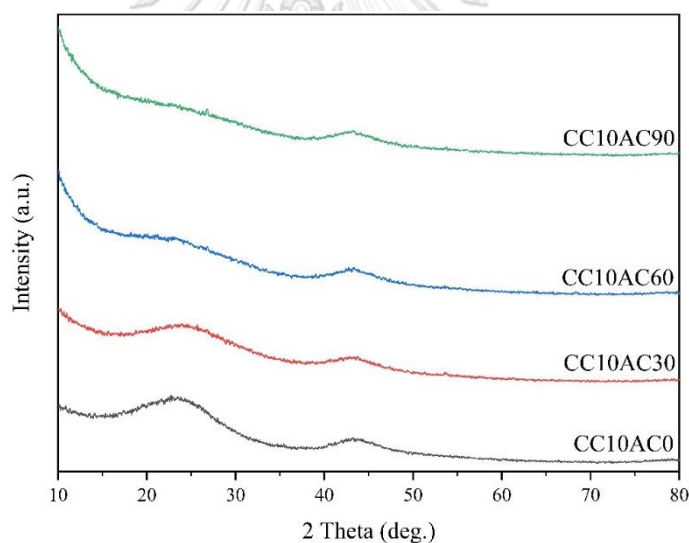


Figure 4.8 XRD patterns of the carbon/carbon composite xerogels obtained under different CO₂ activation time.

4.1.3 Fourier transform infrared analysis

Figure 4.9 illustrates the FTIR spectra of carbon fibers, carbon xerogels, and composites. It can be observed that all the samples have similar surface functional groups. It presents that these samples have nearly the same surface functional groups: the small band at $2900 - 2800 \text{ cm}^{-1}$ is CH_2 stretching vibrations in aliphatic structures. The peaks are observed at $2260 - 2100 \text{ cm}^{-1}$, which can be attributed to $\text{C}\equiv\text{C}$ bonds have formed at the breaking ends[6]. The peaks at 2020 and 1975 cm^{-1} are carbonyl group from quinone group. The band at 1509 cm^{-1} ($\text{C}=\text{C}$ stretching) is the aromatic ring of resorcinol. The band at 1220 cm^{-1} and 1091 cm^{-1} are $\text{CH}_2\text{-O-CH}_2$ linkage group in the phenolic structure. The band at 654 and 746 cm^{-1} ($\text{C}=\text{C}$ bending) is characteristics of $\text{C}=\text{C}$ group vibrations[34]. This indicates that the loading of cotton fibers do not change the surface functional groups.

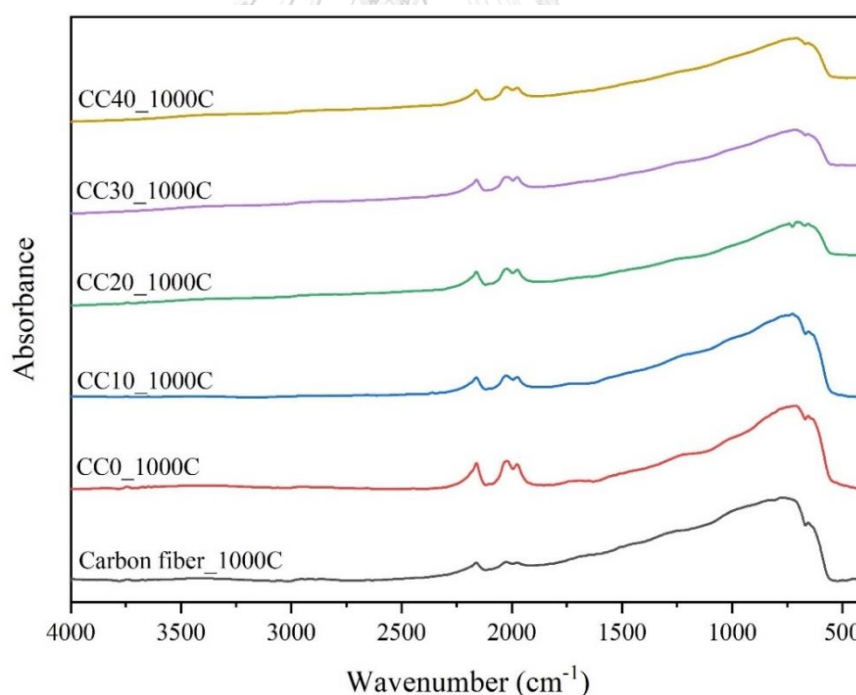


Figure 4.9 FTIR spectra of the carbon/carbon composite xerogels obtained under different content of cotton fibers.

Figure 4.10 shows the FTIR spectra of carbon/carbon composite xerogels were pyrolyzed at various temperature. When carbonization temperature is an increase to

800 °C, the FTIR spectrum slightly changes. The intensity of board peaks at 746 cm^{-1} and 654 cm^{-1} appear more absorbance in samples, which was pyrolysis at 800 to 1000 °C. The result from breaking of the C-O and C-H bonds to C-C bond formation[35]. The peak at 1614 cm^{-1} for aromatic stretching is absent in a sample, which was pyrolysis at 900 °C and 1000 °C. The peaks at 3400 cm^{-1} are referred to OH groups did not appear for the CC10_1000C samples. Due to the pyrolysis temperature of 1000 °C is a minimum pyrolysis temperature to destroy the residual surface functional groups (e.g., OH or hydroxyl group)[7].

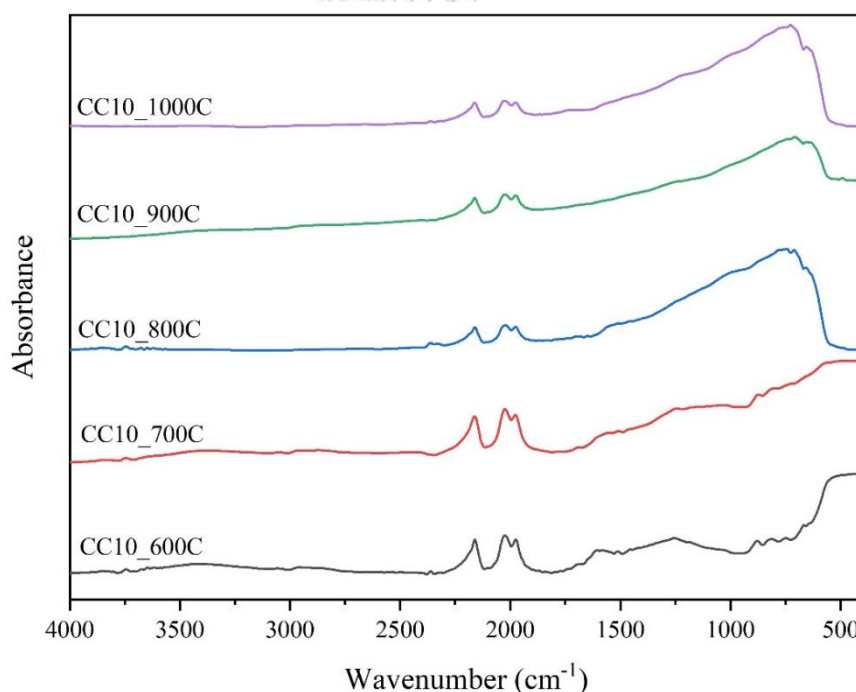


Figure 4.10 FTIR spectra of the carbon/carbon composite xerogels obtained under different carbonization temperature.

Figure 4.11 demonstrates the FTIR spectra of carbon/carbon composite xerogels and activated carbon/carbon composite xerogels. It can be observed that all of the samples have almost similar surface functional groups. After CO_2 activation at 950 °C in 30, 60, and 90 min, the O-H vibration groups appear at 3400 cm^{-1} and C=O vibration groups appear at 2020, and 1975 cm^{-1} compare without CO_2 activation[36]. For the O-H groups and C=O groups, its intensity for the CC10AC30, CC10AC60, and

CC10AC90 were stronger than the CC10_1000C samples. This indicates that a higher content of O–H groups and C=O groups were produced during the CO₂ activation process[37].

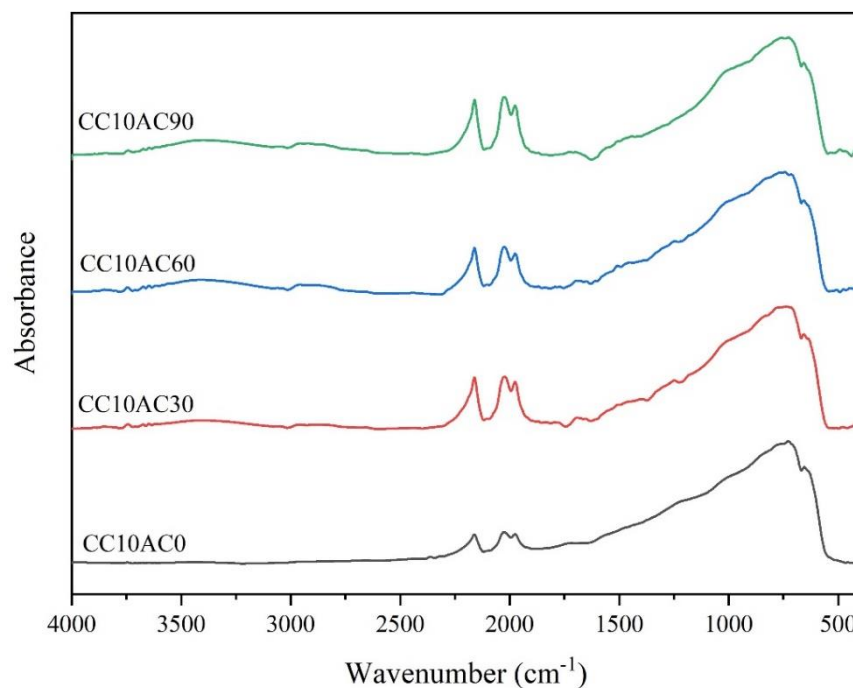


Figure 4.11 FTIR spectra of the carbon/carbon composite xerogels obtained under different CO₂ activation time.

4.1.4 Surface area and porosity analysis

The porous properties of the carbon/carbon composite xerogels show in Figure 4.12 and Table 4.1. Table 4.1 presents the BET surface area of the carbon/carbon composite xerogels ranges from 625 – 514 m²/g. The surface area of the samples was decreased slightly when increasing the content of cotton fibers to the resorcinol-formaldehyde gels matrix. The nitrogen adsorption-desorption isotherms of samples shown in Figure 4.12. All of the samples exhibit a type IV isotherm. The isotherms of samples present the fast increase at low relative pressures and the hysteresis loops at high relative pressures, indicating the presence of micropores and mesopores, respectively[5]. The carbon fibers from cotton fibers show type I isotherms and

exhibited mainly no hysteresis loop (in Figure 4.12), indicating that carbon fibers have a main microporous structure. The hysteresis loops of carbon/carbon composite xerogels are narrow at high relative pressure. These indicate that the carbon/carbon composite xerogels have a large mesopore diameter[4]. Table 4.1 shows the mesopore volume and pore diameter of the carbon/carbon composite xerogels with and without cotton fibers. The carbon/carbon composite xerogels with 40 wt.% cotton fibers (CC40_1000C) have mesopore volume and pore diameter than the sample with 30 wt.% cotton fibers, 20 wt.% cotton fibers, 10 wt.% cotton fibers and 0 wt.% cotton fibers, respectively. These indicate that the mesopore volume and pore diameter increase when the content of cotton fibers increase. Figure 4.13 shows BJH mesopore size distribution of samples. CC0_1000C has a narrow mesopore size distribution curve. When the content of cotton fibers is increased, the mesopore size distribution of carbon/carbon composite xerogels are developed[5].

Table 1 Porous properties of the carbon/carbon composite xerogels obtained under different of cotton fibers at a carbonization temperature of 1000 °C

Sample	S_{BET} (m^2/g)	V_{micro} (cm^3/g)	V_{meso} (cm^3/g)	d_p (nm)	V_{total} (cm^3/g)
Carbon fiber_1000C	440	0.2673	0.095374	2.52	0.3210
CC0_1000C	625	0.3426	1.0567	16.39	1.2338
CC10_1000C	575	0.3075	1.1209	18.92	1.2785
CC20_1000C	598	0.3295	1.2226	18.92	1.3947
CC30_1000C	562	0.2805	1.1967	18.92	1.3363
CC40_1000C	514	0.3167	1.3475	18.92	1.5165

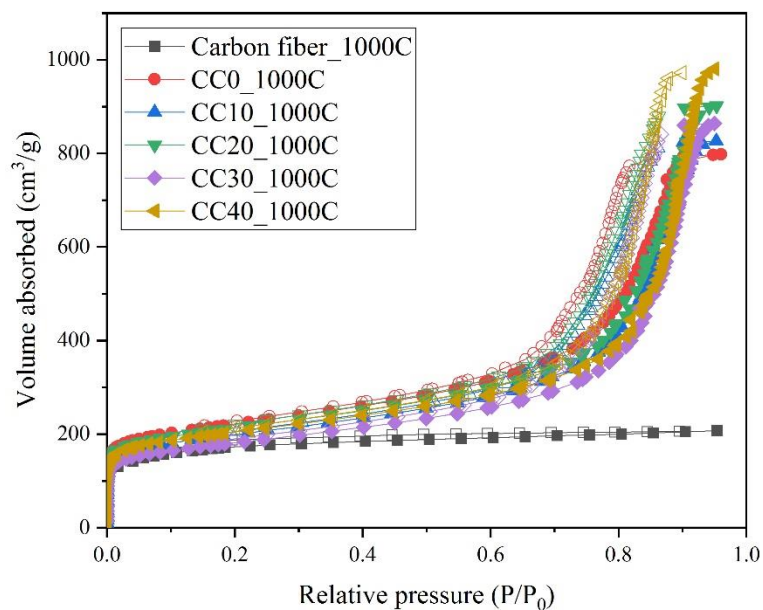


Figure 4.12 Nitrogen adsorption-desorption isotherms of carbon/carbon composite xerogels obtained under a pyrolysis temperature of 1000 °C and different content of cotton fibers.

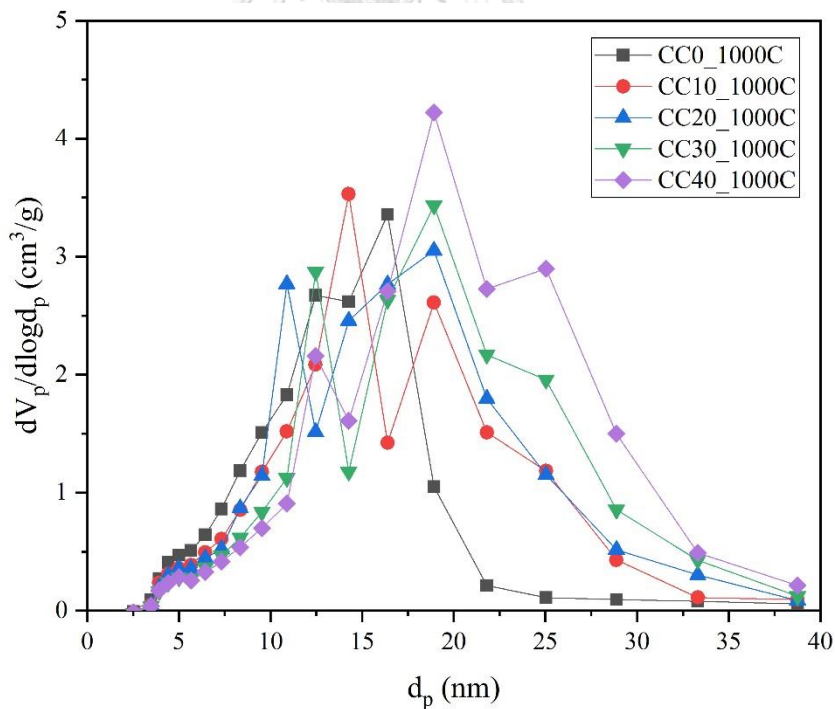


Figure 4.13 BJH pore size distribution for carbon/carbon composite xerogels obtained under different content of cotton fibers.

The porous properties of the carbon/carbon composite xerogels with 10wt.% cotton fibers after pyrolyzed at a various pyrolysis temperature shown in Figure 4.14 and Table 4.2. Table 4.2 presents the specific surface area (S_{BET}) of the carbon/carbon composite xerogels ranges from 625 – 598 m^2g^{-1} . The specific surface area (S_{BET}) of the samples was decreased slightly when increasing the pyrolysis temperatures. The nitrogen adsorption-desorption isotherms of samples shown in Figure 4.14. All of the samples exhibit a type IV isotherm, indicating the presence of micropores and mesopores, respectively[5]. Table 4.2 shows the micropore volume, mesopore volume and pore diameter of the carbon/carbon composite xerogels with 10wt.% cotton fibers. The CC10_1000C had micropore volume, mesopore volume and pore diameter than CC10_900C, CC10_800C, CC10_700C, and CC10_600C, respectively. These indicate that the micropore volume, mesopore volume, and pore diameter increase when increasing the pyrolysis temperatures. Figure 4.15 shows the BJH mesopore size distribution of samples. All of the samples had a nearly mesopore size distribution curve.

Table 2 Porous properties of the carbon/carbon composite xerogels obtained under different pyrolysis temperature at a content of 10 wt% cotton fibers

Sample	S_{BET} (m^2/g)	V_{micro} (cm^3/g)	V_{meso} (cm^3/g)	d_p (nm)	V_{total} (cm^3/g)
CC10_600C	625	0.3453	1.0334	12.46	1.2216
CC10_700C	613	0.3408	1.0832	16.39	1.2679
CC10_800C	578	0.3185	1.0383	16.39	1.2104
CC10_900C	590	0.3225	1.1036	18.92	1.2679
CC10_1000C	575	0.3075	1.1209	18.92	1.2785

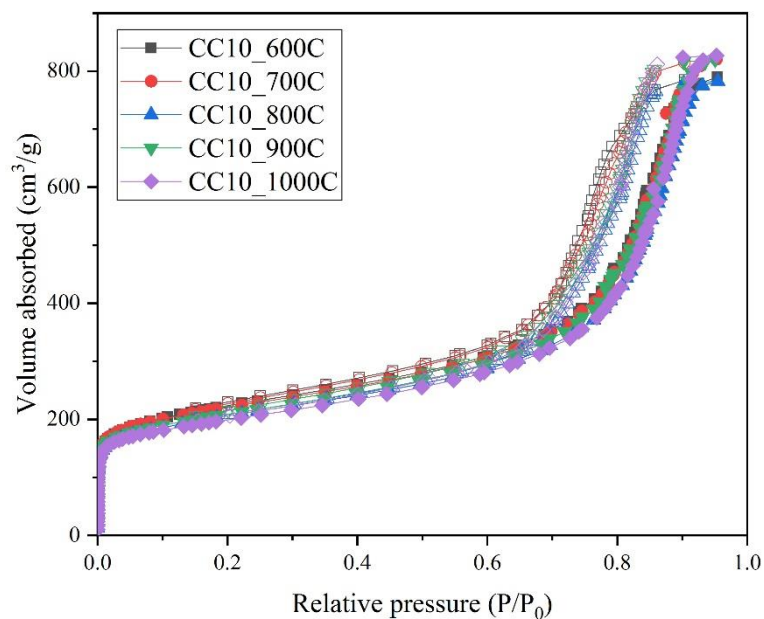


Figure 4.14 Nitrogen adsorption-desorption isotherms of carbon/carbon composite xerogels obtained under different pyrolysis temperature.

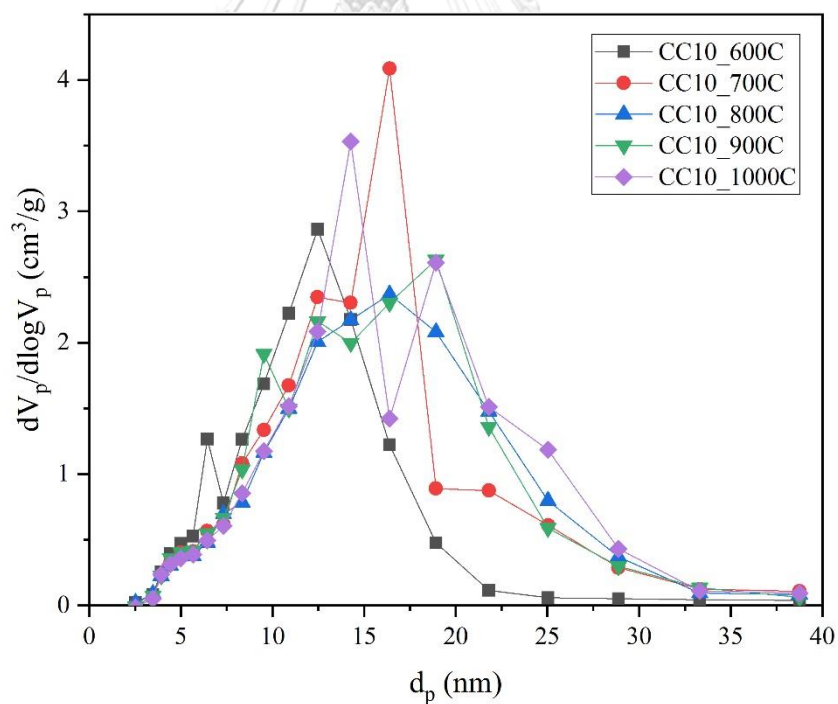


Figure 4.15 BJH pore size distribution for carbon/carbon composite xerogels obtained under different pyrolysis temperature.

Table 4.3 illustrates the porous properties of the carbon/carbon composite xerogels prepared after activation with CO₂ have an increased both the specific surface area (S_{BET}) and the micropore volume compare to pyrolyzed carbon/carbon composite xerogels without CO₂ activation. For the activated carbon/carbon composite xerogels with CO₂ activation time ranging from 0 to 90 min, specific surface area (S_{BET}) increases from 562 m² g⁻¹ (CC10_1000C) to 1471 m² g⁻¹ (CC10AC90), while micropore volume increases from 0.75 to 1.74 cm³ g⁻¹, respectively. Figure 4.16 demonstrates the N₂ adsorption-desorption isotherms of activated carbon/carbon composite xerogels with 10 wt.% cotton fibers at 950 °C during 0, 30, 60 and 90 min of CO₂ activation times. All of the isotherms is a type IV isotherm, which resembles micropore and mesopore in samples. CO₂ activation time induces an increase of N₂ adsorption at low relative pressure are shift upwards when CO₂ activation time increased. This indicates that CO₂ activation develops micropores. The hysteresis loops changed at high relative pressure when CO₂ activation time increased. These indicate that the CO₂ activation modifies both the mesoporosity and the microporosity[10].

Table 3 Porous properties of the carbon/carbon composite xerogels obtained under different CO₂ activation time at a content of 0 and 10 wt% cotton fibers

Sample	%Burn off	S_{BET} (m ² /g)	V_{micro} (cm ³ /g)	V_{meso} (cm ³ /g)	d_p (nm)	V_{total} (cm ³ /g)
CC0_1000C	-	625	0.3426	1.0567	16.39	1.2338
CC0AC30	16.84	801	0.4728	0.9265	10.89	1.2015
CC0AC60	20.02	937	0.6528	1.0121	12.46	1.3054
CC0AC90	37.80	1116	0.8601	1.3451	16.39	1.7738
CC10_1000C	-	575	0.3075	1.1209	18.92	1.2785
CC10AC30	32.05	954	0.6002	1.6047	18.92	1.9992
CC10AC60	37.38	1092	0.6393	1.5757	18.92	2.0080
CC10AC90	49.75	1471	0.8601	2.0553	18.92	2.6247

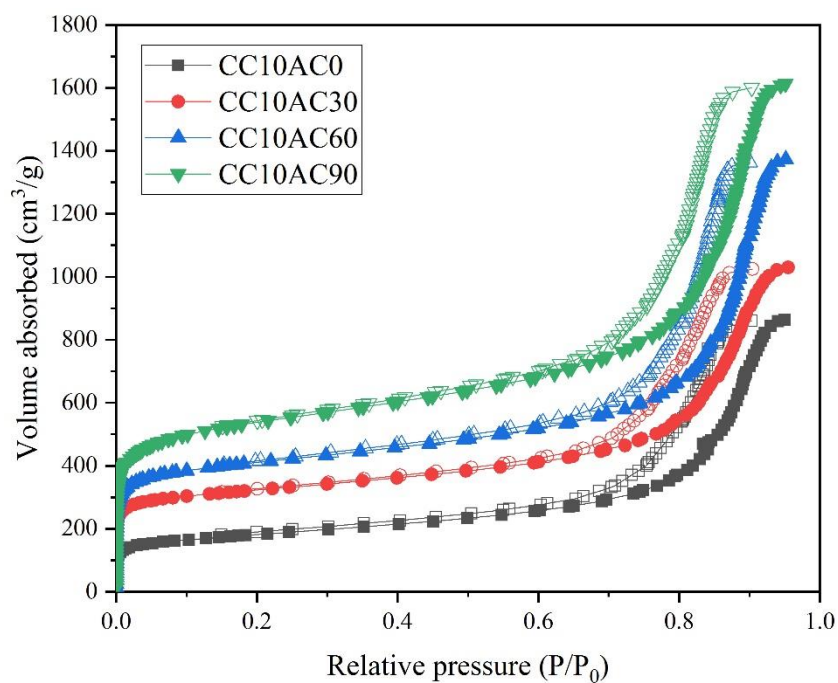


Figure 4.16 Nitrogen adsorption-desorption isotherms of carbon/carbon composite xerogels obtained under different CO_2 activation time.

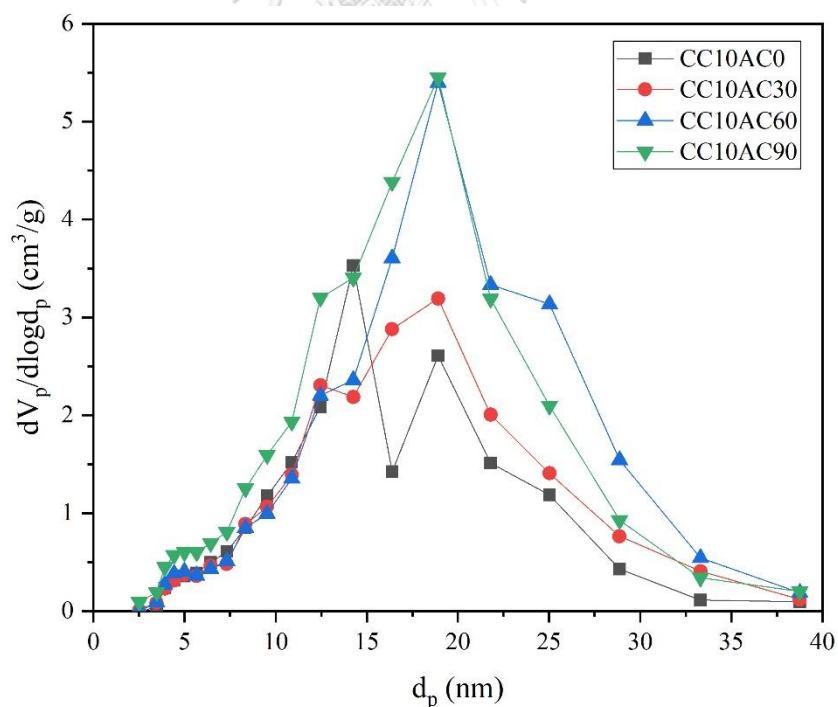


Figure 4.17 BJH pore size distribution for activated carbon/carbon composite xerogels obtained under different CO_2 activation time.

After the CO₂ activation process at 90 min, Comparing between carbon xerogels without cotton fibers (CC0AC90) and carbon/carbon composite xerogels with cotton fibers (CC10AC90). The activated carbon/carbon composite xerogels with cotton fibers have a higher BET surface area, both micropore, and mesopore volume and pore diameter than activated carbon xerogels without cotton fibers. This indicates that the presence of cotton fibers is essential for obtaining a high surface area in the same CO₂ activation time compare without cotton fibers. Due to the addition of cotton fibers in carbon xerogels to change the mesopore larger than carbon xerogels without cotton fibers.

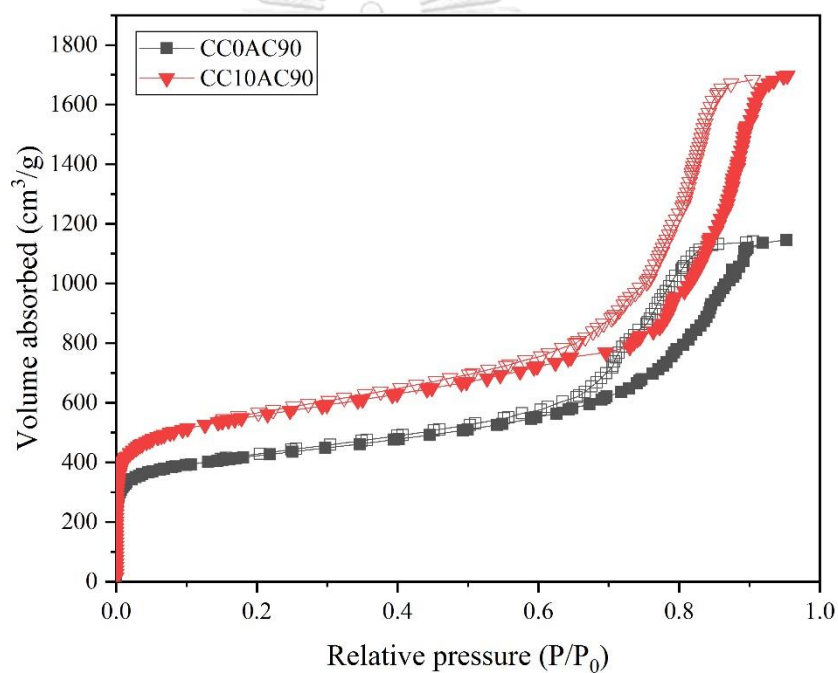


Figure 4.18 Nitrogen adsorption-desorption isotherms of carbon/carbon composite xerogels obtained under a CO₂ activation 90 min using with and without cotton fibers.

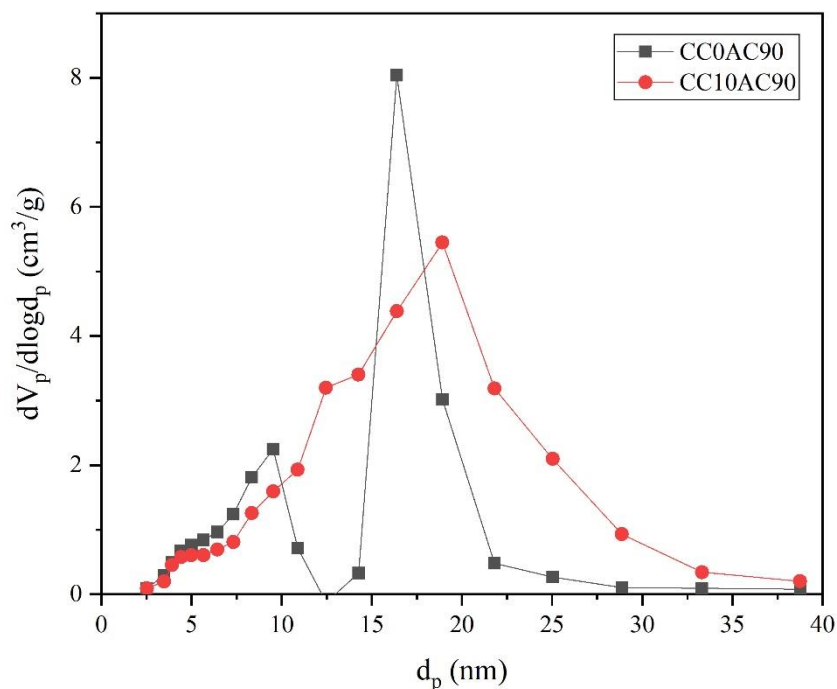


Figure 4.19 BJH pore size distribution for activated carbon/carbon composite xerogels obtained under a CO₂ activation 90 min using with and without cotton fibers.

4.2 Electrochemical performances of carbon/carbon composite xerogels electrodes

4.2.1 Effect of % cotton fibers loading

Figure 4.20 shows cyclic voltammetry curves of CC0_1000C, CC10_1000C, CC20_1000C, CC30_1000C and CC40_1000C were measured in 4M KOH solution at 3 mV s⁻¹ of the scan rate. The cyclic voltammograms of all samples have a nearly-rectangular shape with no reduction and oxidation peaks, indicating that the samples demonstrate electrical double-layer behavior. The specific capacitances of CC0_1000C, CC10_1000C, CC20_1000C, CC30_1000C and CC40_1000C from cyclic voltammograms are shown in Figure 4.21. It turned out that the capacitance increased with %cotton fibers to 10 wt.% and decreased with %cotton fibers 20 wt.%, 30 wt.% and wt.40%, respectively. The highest specific capacitance (179 F g⁻¹)

was obtained with the carbon/carbon composite xerogels with 10 wt.% cotton fibers at scan rate 3 mV s^{-1} . This result indicated that cotton fibers added to carbon/carbon composites xerogels which can increase the specific capacitance of EDLCs because the carbon tunnels of carbon/carbon composite xerogels promote the mass transport of electrolyte ions into the pore[4].

Figure 4.22 shows the cyclic voltammograms at the different scan rates of CC10_1000C (10wt% cotton fibers) electrodes. The specific capacitances of CC10_1000C at 3, 5, 10, 30, 50, 100 and 500 mVs^{-1} from cyclic voltammetry curves were calculated to be 179 F g^{-1} , 140 F g^{-1} , 84 F g^{-1} , 22 F g^{-1} , 10 F g^{-1} , 4 F g^{-1} and 0.4 F g^{-1} , respectively. The specific capacitance decreases when the scan rate increases, because of the kinetics effects and weak electrolyte ions diffusion into the micropores at higher scan rates[38].

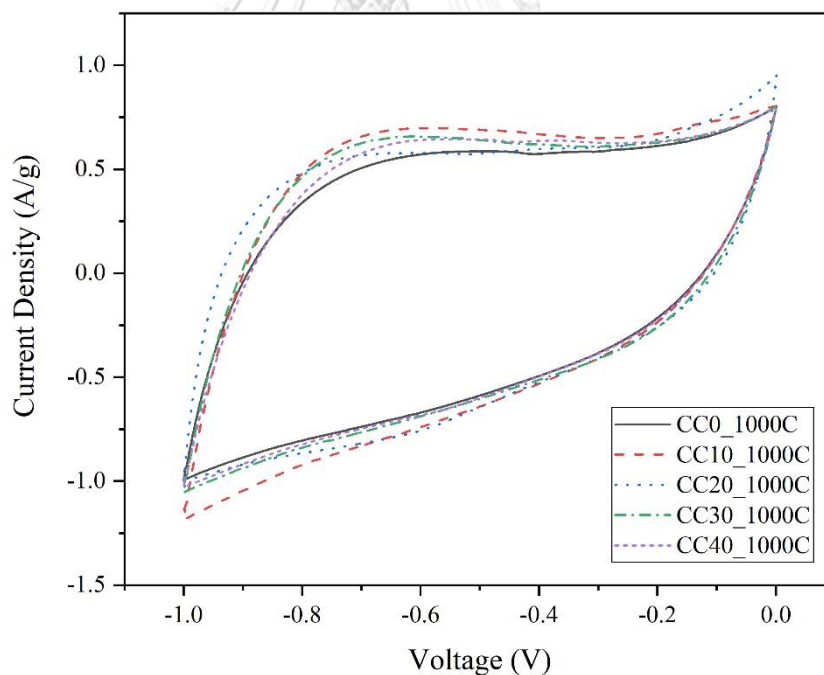


Figure 4.20 Cyclic voltammetry curves of the carbon/carbon composite xerogel electrodes at a scan rate of 0.3 mV s^{-1} in 4M KOH.

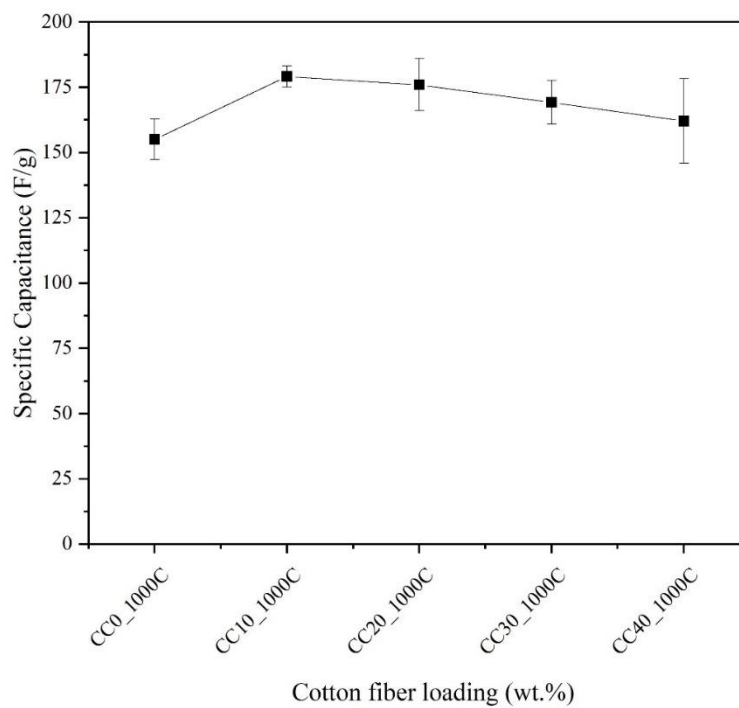


Figure 4.21 specific capacitance from cyclic voltammograms of the carbon/carbon composite xerogel electrodes obtained under different content of cotton fibers. at a scan rate of 0.3 mV s^{-1} in 4M KOH.

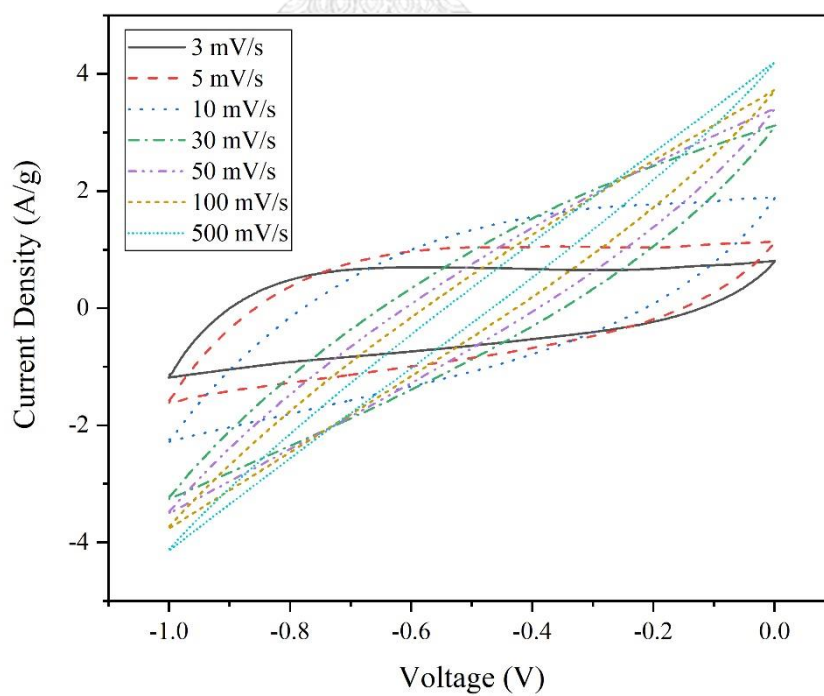


Figure 4.22 Cyclic voltammetry curves of CC10_1000C electrodes at different scan rates using in 4M KOH.

The galvanostatic charge-discharge of the carbon/carbon composites xerogels at 0.5 A g^{-1} of the current density shows an almost triangular shape, indicating symmetry between charge and discharge (Figure 4.23). The specific capacitances of CC0_1000C, CC10_1000C, CC20_1000C, CC30_1000C, and CC40_1000C from discharge curves are shown in Figure 4.24, which supports the result obtained in cyclic voltammetry measurement. The specific capacitances of CC0_1000C at 0.5, 1, 1.5 and 2 A g^{-1} from discharge curves (Figure 4.25) were calculated to be 144 F g^{-1} , 113 F g^{-1} , 100 F g^{-1} and 91 F g^{-1} , respectively. The results confirm that the increase of the current density will decrease the charge-discharge time.

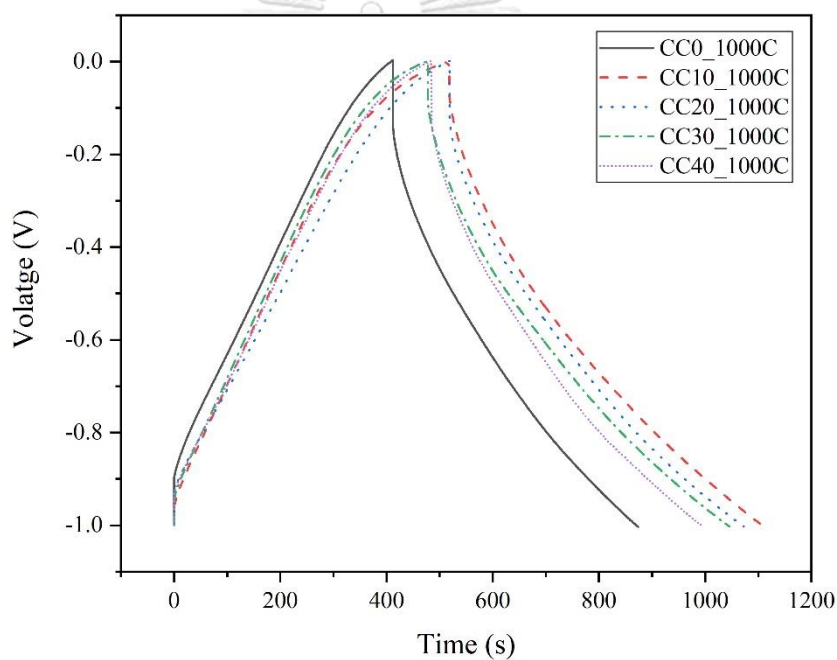


Figure 4.23 Galvanostatic charge-discharge curves of the carbon/carbon composite xerogel electrodes at a current density of 0.5 A g^{-1} in 4M KOH.

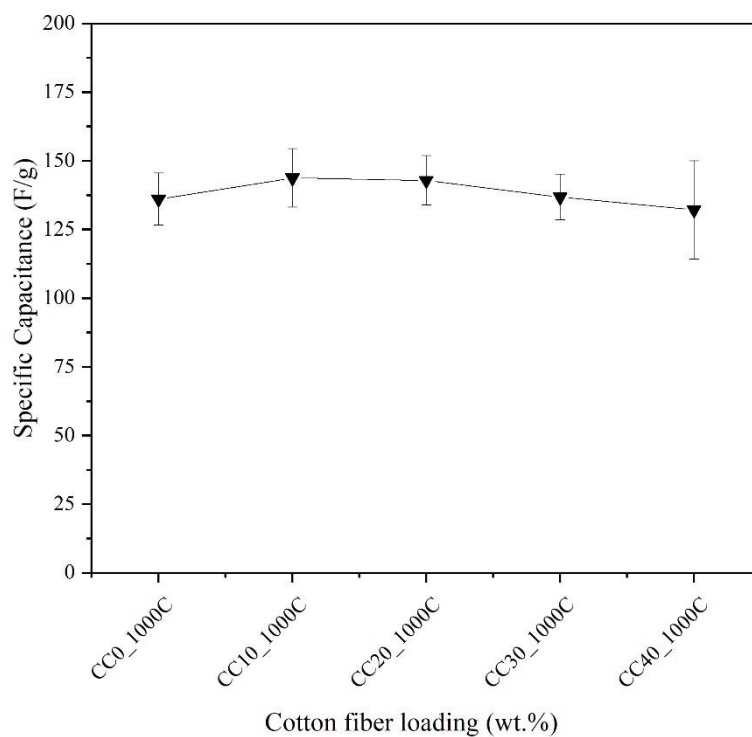


Figure 4.24 specific capacitance from discharge curves of the carbon/carbon composite xerogel electrodes obtained under different content of cotton fibers at a scan rate of 0.3 mV s^{-1} in 4M KOH .

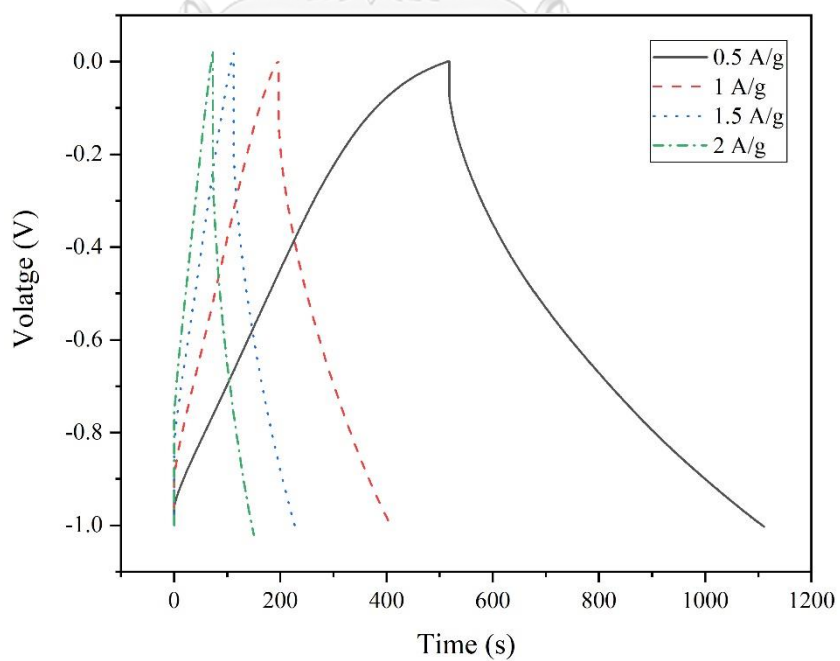


Figure 4.25 Galvanostatic charge-discharge curves of CC10_1000C electrodes at different current density using in 4M KOH .

4.2.2 Effect of various pyrolysis temperatures

After optimizing the content of cotton fibers, the pyrolysis temperature of the carbon/carbon composite xerogels with 10wt.% cotton fibers was further optimized in the range of 600–1000 °C. Figure 4.26 shows cyclic voltammetry curves of CC10_600C, CC10_700C, CC10_800C, CC10_900C, and CC10_900C were measured in 4M KOH solution at 3 mV s⁻¹ of the scan rate. The cyclic voltammograms of all samples have a nearly-rectangular shape with the absence of redox reaction, indicating that the samples demonstrate electrical double-layer behavior[30]. The effect of different pyrolysis temperatures on the specific capacitance from cyclic voltammograms of the samples shown in Figure 4.27. The specific capacitances of CC10_600C, CC10_700C, CC10_800C, CC10_900C, and CC10_1000C from cyclic voltammogram were calculated to be 7, 116, 174, 175, and 179 F g⁻¹, respectively. It shows that the specific capacitance increased as the pyrolysis temperature increases. The specific capacitance values of the carbon/carbon composite xerogels pyrolyzed at 800 to 1000 °C are not changed significantly as shown in Figure 4.27. The increase of the specific capacitance with pyrolysis temperature increased can be explained on XRD patterns (Figure 4.7) and the resistance values (Figure 4.28). The XRD patterns illustrate that the carbon/carbon composites xerogels have more graphite region after increase pyrolysis temperature from 600 to 1000 °C. The resistance values support this. Figure 4.28 shows the resistance of samples prepared at pyrolysis temperature of 600, 700, 800, 900 and 1000 °C. When the pyrolysis temperature increase from 600 °C to 1000 °C, the resistance dropped from 2.72 megaohms to 9.1 ohms. These confirm that the pyrolysis temperature effects on the conductivity of carbon/carbon composite xerogels.

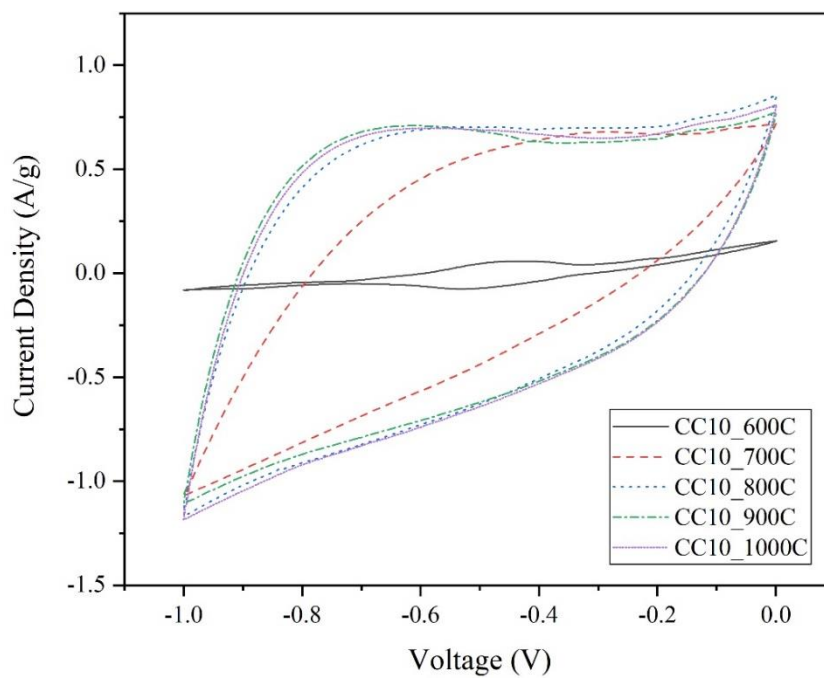


Figure 4.26 Cyclic voltammograms of the carbon/carbon composite xerogel electrodes obtained under different pyrolysis temperature at a scan rate of 0.3 mV s^{-1} in 4M KOH.

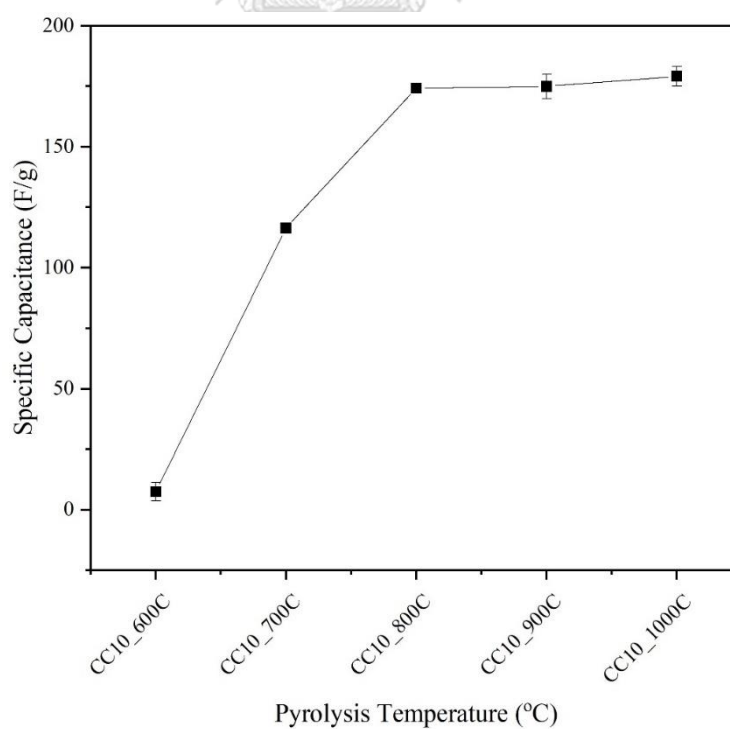


Figure 4.27 Specific capacitance from cyclic voltammogram of carbon/carbon composite xerogels obtained under different pyrolysis temperatures

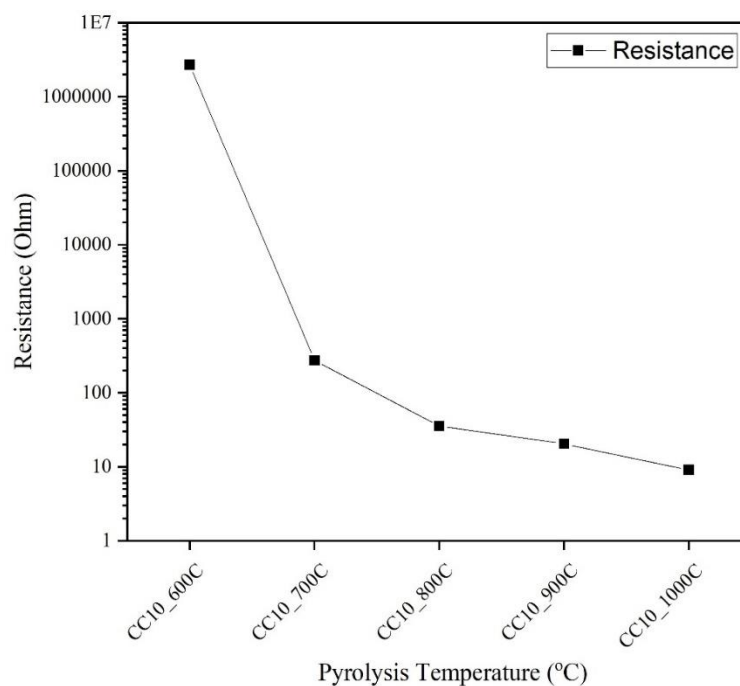


Figure 4.28 resistance value of carbon/carbon composite xerogels obtained under different pyrolysis temperatures

The galvanostatic charge-discharge of the carbon/carbon composites xerogels at 0.5 Ag^{-1} of the current density shows an almost triangular shape, indicating symmetry between charge and discharge (Figure 4.29). The specific capacitances of CC10_600C, CC10_700C, CC10_800C, CC10_900C, and CC10_1000C from discharge curves are shown in Figure 4.30, which supports the result obtained in cyclic voltammetry measurement.

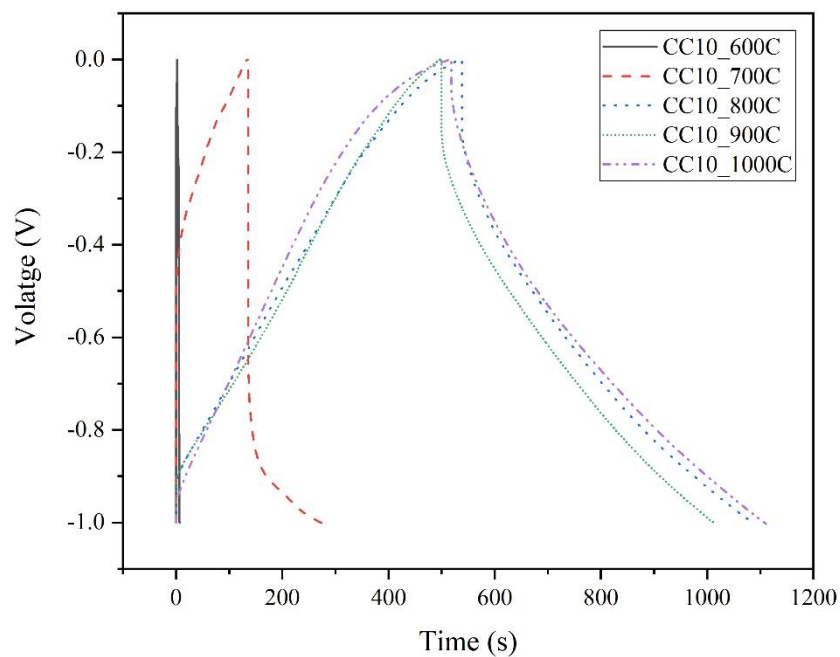


Figure 4.29 Galvanostatic charge-discharge curves of the carbon/carbon composite xerogel electrodes obtained under different pyrolysis temperature at a scan rate of 0.3 mV s^{-1} in 4M KOH.

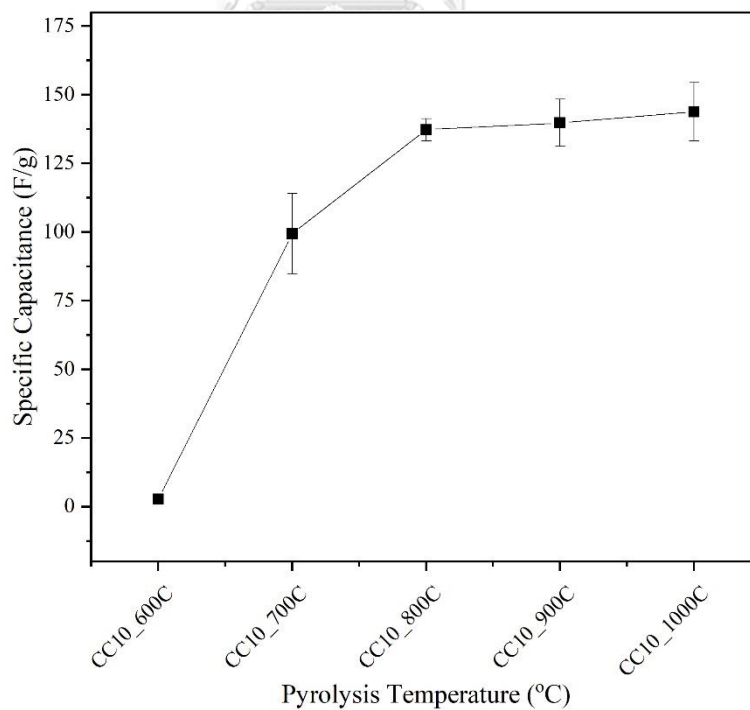


Figure 4.30 Specific capacitance from discharge curves of carbon/carbon composite xerogels obtained under different pyrolysis temperatures

4.2.3 Effect of CO₂ activations

The electrochemical performance of the activated carbon/carbon composite xerogels was investigated. Figure 4.31 shows the cyclic voltammogram of carbon/carbon composite xerogels with 10 wt.% cotton fiber loading at different CO₂ activation time. After activated with CO₂, All of the samples (CC10AC30, CC10AC60, and CC10AC90) demonstrated distorted rectangular cyclic voltammogram shapes with reduction and oxidation peaks, which indicated the occurrence of a redox pseudocapacitive reaction caused by oxygen functional groups at 3 mV s⁻¹, as shown in Figure 4.31 [39, 40]. Oxygen functional groups, such as carbonyl groups (C=O) and hydroxyl groups (O-H), was introduced on the carbon/carbon composite xerogels via CO₂ activation process[37]. The effect of different CO₂ activation time on the specific capacitance from the cyclic voltammograms of the samples shown in Figure 4.32. The specific capacitances of CC0_1000C, CC0AC30, CC0AC60, and CC0AC90 from cyclic voltammogram were calculated to be 155, 171, 185, and 202 Fg⁻¹, respectively. In addition, The specific capacitances of CC10_1000C, CC10AC30, CC10AC60, and CC10AC90 from cyclic voltammogram were calculated to be 179, 197, 218, and 251 Fg⁻¹, respectively. It shows that the specific capacitance increased as the CO₂ activation time increases. This results can be explained after looking at the specific surface area (S_{BET}) (Table 3) and the surface functional groups observed in FTIR (Figure 4.11). It shows that the specific surface area (S_{BET}) increased with the CO₂ activation time increased. Moreover, It is seen that the absorbance peaks of hydroxyl groups (O-H) and carbonyl groups (C=O) increased with the CO₂ activation time increased. Furthermore, the activated carbon/carbon composite xerogels with 10wt.% cotton fibers had a specific capacitance from cyclic voltammogram higher than the activated carbon xerogels without cotton fibers.

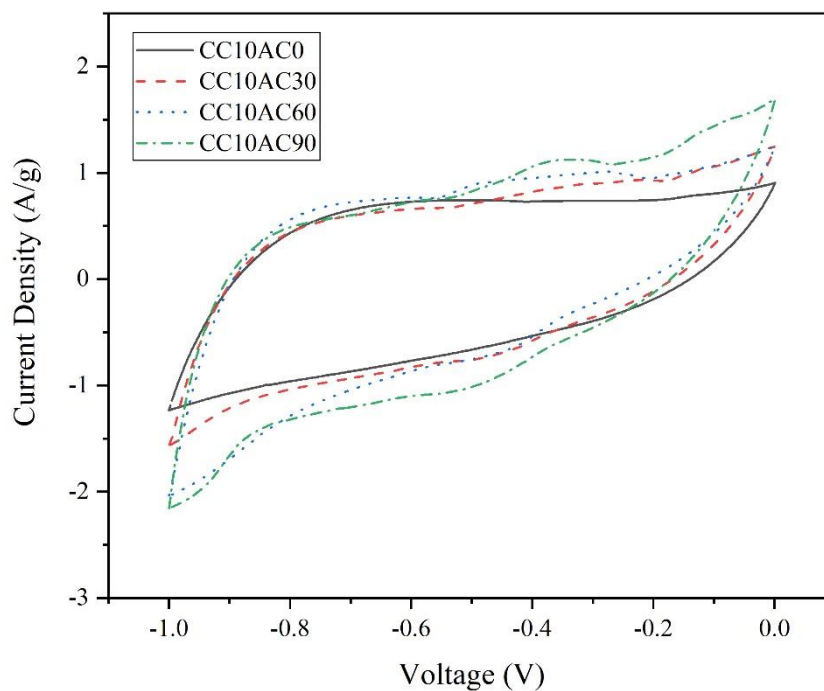


Figure 4.31 Cyclic voltammetry curves of the carbon/carbon composite xerogel electrodes obtained under different CO_2 activation time at a scan rate of 0.3 mV s^{-1} in 4M KOH.

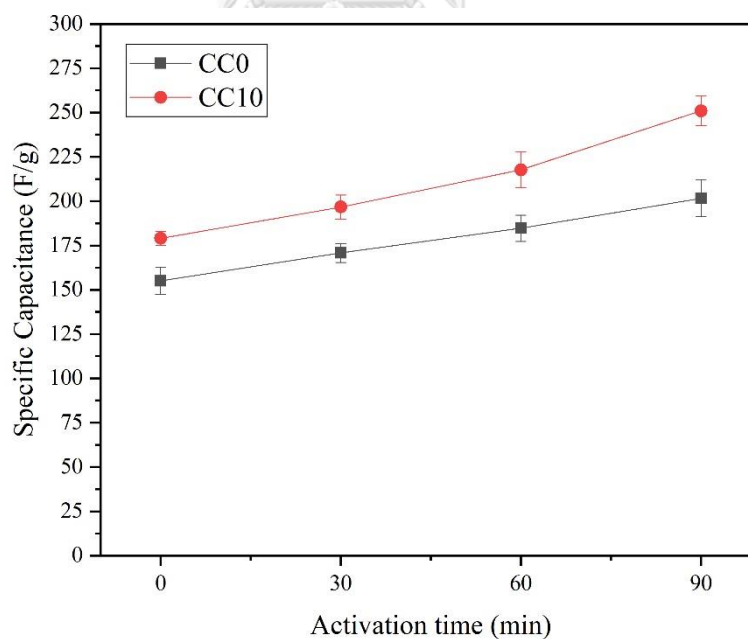


Figure 4.32 Specific capacitance from cyclic voltammogram of carbon/carbon composite xerogels obtained under different CO_2 activation time

Figure 4.33 **Figure 4.22** shows the cyclic voltammograms at the different scan rates of CC10AC90 electrodes. The specific capacitances of CC10AC90 at 3, 5, 10, 30, 50, 100 and 500 mVs^{-1} from cyclic voltammetry curves were calculated to be 251 F g^{-1} , 187 F g^{-1} , 118 F g^{-1} , 39 F g^{-1} , 20 F g^{-1} , 8 F g^{-1} and 0.8 F g^{-1} , respectively. The specific capacitance decreases when the scan rate increases, because of the kinetics effects and weak electrolyte ions diffusion into the micropores at higher scan rates[38].

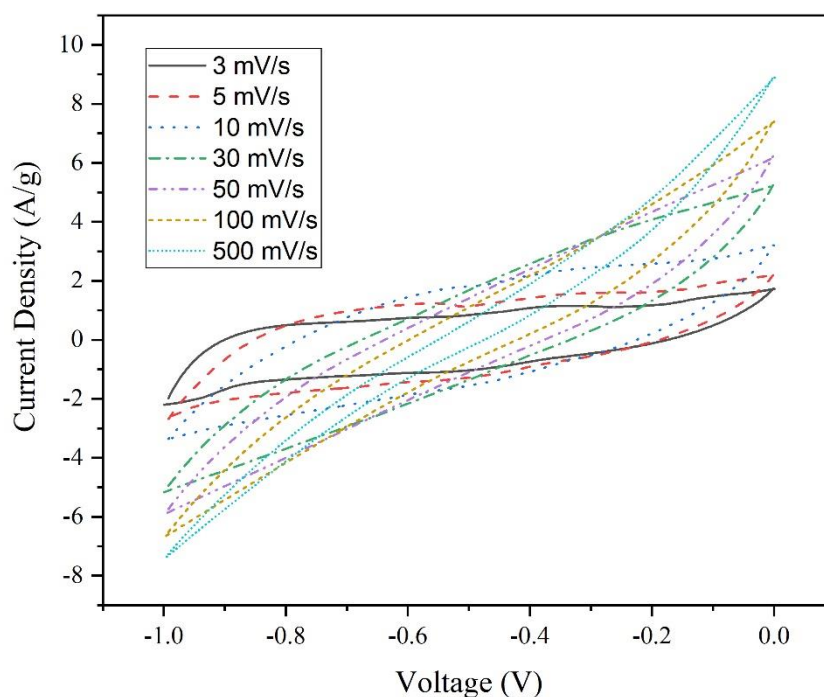


Figure 4.33 Cyclic voltammograms of CC10AC90 electrodes at different scan rates using in 4M KOH

Figure 4.34 illustrates the galvanostatic charge-discharge curves of carbon/carbon composite xerogels (CC10_1000C) and activated carbon/carbon composite xerogels (CC10AC30, CC10AC60, and CC10AC90), which shows an almost symmetrical curve, indicating symmetry between charge and discharge. The rugged charge-discharge curves can be negligible of all the activated carbon/carbon composite xerogels, which shows the redox reaction of these activated samples. The specific capacitances of samples from discharge curves are shown in Figure 4.35, which supports the result obtained in cyclic voltammetry measurement. Figure 4.35

shows the highest specific capacitance (344 F g^{-1} at 0.5 A g^{-1}) for 10 wt.% of cotton fibers loaded resorcinol-formaldehyde gels with at CO_2 activation 90 min, which is much higher than the for 10 wt.% of cotton fibers loaded resorcinol-formaldehyde gels without CO_2 activation (144 F g^{-1} at 0.5 A g^{-1}). Furthermore, The specific capacitances of CC10AC90C at 0.5, 1, 1.5 and 2 A g^{-1} from discharge curves (Figure 4.36) were calculated to be 344 F g^{-1} , 259 F g^{-1} , 213 F g^{-1} , and 169 F g^{-1} , respectively.

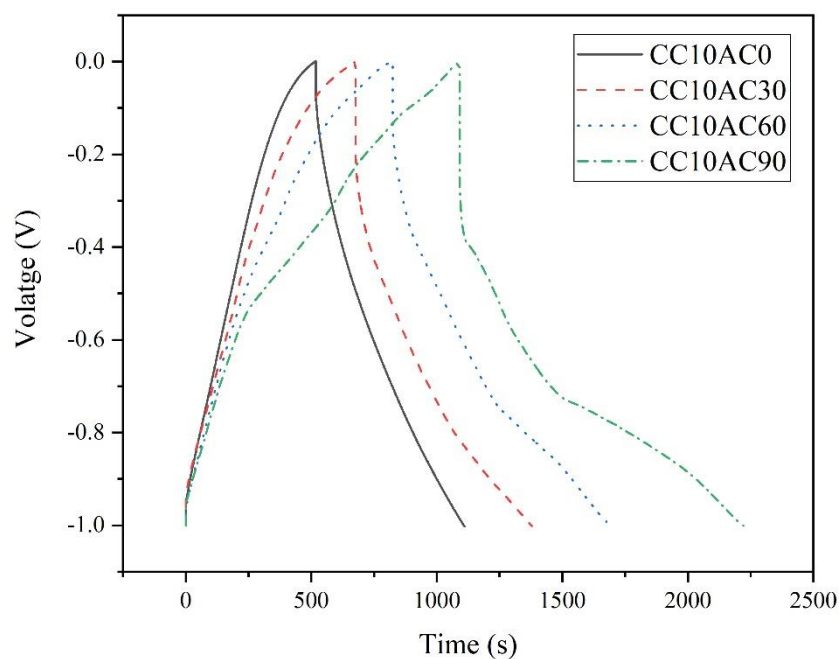


Figure 4.34 Galvanostatic charge-discharge curves of the carbon/carbon composite xerogel electrodes obtained under different CO_2 activation time at a scan rate of 0.3 mV s^{-1} in 4M KOH

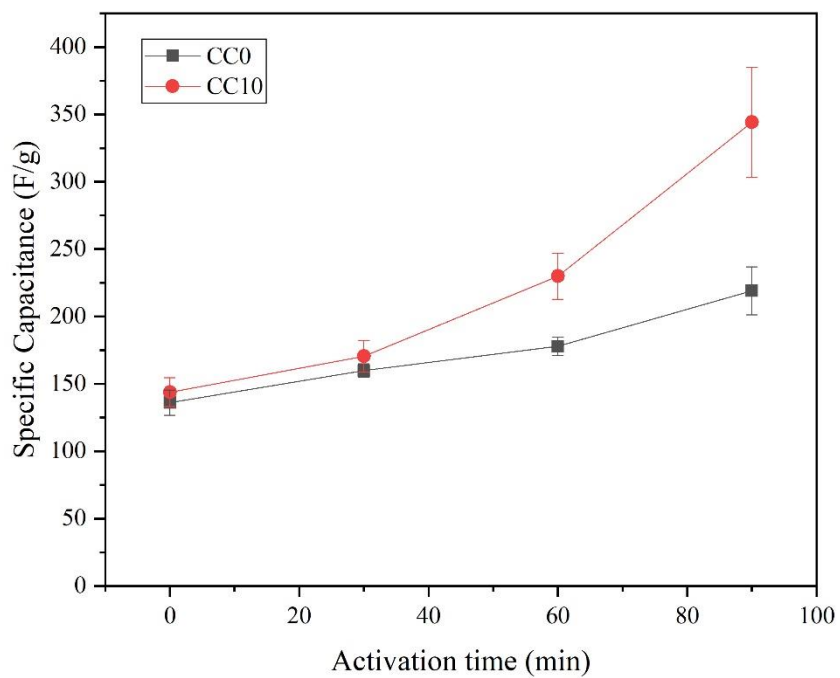


Figure 4.35 Specific capacitance from discharge curves of carbon/carbon composite xerogels obtained under different CO₂ activation time

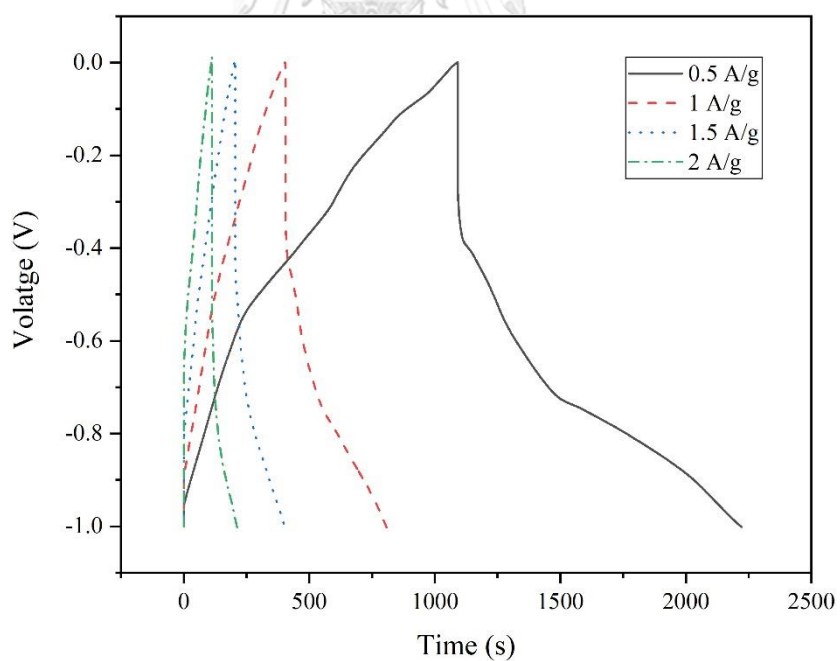


Figure 4.36 Galvanostatic charge-discharge curves of CC10AC90 electrodes at different current density using in 4M KOH

From many studied effects in this research, the electrodes were synthesized from resorcinol-formaldehyde resins, contained 10 wt.% cotton fibers, pyrolyzed at 1000 °C, and activated with CO₂ 90 min gave the highest specific capacitance from cyclic voltammogram and discharge curve more than other carbon/carbon composite xerogels.



CHAPTER 5

CONCLUSIONS

5.1 Conclusions

This research synthesized the carbon/carbon composite xerogels for use as an electrode for electrical double layer capacitors (EDLCs) which focused on the effect of different % cotton fibers loading on resorcinol-formaldehyde gels matrix, pyrolysis temperatures and CO₂ activation times.

The carbon/carbon composite xerogels were prepared through polycondensation polymerization between resorcinol-formaldehyde and cotton fibers as a carbon-based precursor. In the carbon/carbon composite xerogels, percentage of cotton fibers was varied at 0, 10, 20, 30, and 40 wt.%. The carbon/carbon composite xerogels were pyrolyzed at various temperatures (600, 700, 800, 900 and 1000 °C) under N₂ atmosphere and were activated at 950 °C with CO₂ activations (30, 60, 90 min). The electrochemical performance of carbon/carbon composite xerogels was measured by the cyclic voltammetry and the galvanostatic charge-discharge mode. The optimum content of cotton fibers for optimal performance is 10 wt.% cotton fibers loading. The surface area of the samples was decreased slightly when increasing the content of cotton fibers. Nevertheless, cotton fibers added to carbon/carbon composites xerogels which can increase the specific capacitance of EDLCs. Moreover, the pyrolysis temperature study showed that for these carbon/carbon composite xerogels, a temperature of about 800 to 1000 °C appeared to be optimum. Furthermore, the presence of cotton fibers is essential for obtaining a high surface area in the same CO₂ activation time compare without cotton fibers. CO₂ activation enhanced the porous properties of carbon/carbon composite xerogels such as specific surface area (S_{BET}), micropore volume and mesopore volume; therefore, these effects affected carbon/carbon composite xerogel electrodes to high specific capacitance.

For electrochemical performance, CC10AC90 performed the highest specific capacitance from cyclic voltammogram and discharge curve of 251 F g^{-1} at 3 mV s^{-1} and 344 F g^{-1} at 0.5 A g^{-1} , respectively.

5.2 Recommendations

Base on what has been discovered in this research, the following recommendations were suggested:

- The prepared samples should be a measure of mechanical properties such as compression, tensile strength.
- The prepared samples should be tested electrochemical performance in the organic electrolytes to study the effect of electrolytes on the specific capacitance of electrodes.
- The prepared samples should be activated with steam to study the effect of physical activation on the porous properties of electrodes.

REFERENCES

1. Ramos-Fernández, G., et al., *Determinant influence of the electrical conductivity versus surface area on the performance of graphene oxide-doped carbon xerogel supercapacitors*. Carbon, 2018. **126**: p. 456-463.
2. Ratajczak, P., et al., *Carbon electrodes for capacitive technologies*. Energy Storage Materials, 2019. **16**: p. 126-145.
3. PEKALA, R.W., *Organic aerogels from the polycondensation of resorcinol with formaldehyde*. JOURNAL OF MATERIALS SCIENCE, 1989. **24**: p. 3221-3227.
4. Kraiwattanawong, K., N. Sano, and H. Tamon, *Capacitive performance of binder-free carbon/carbon composite cryogels*. Microporous and Mesoporous Materials, 2013. **165**: p. 228-233.
5. Kraiwattanawong, K., N. Sano, and H. Tamon, *Low-cost production of mesoporous carbon/carbon composite cryogels*. Carbon, 2011. **49**(11): p. 3404-3411.
6. Hebalkar, N., et al., *Study of correlation of structural and surface properties with electrochemical behaviour in carbon aerogels*. Journal of Materials Science, 2005. **40**(14): p. 3777-3782.
7. Lin, C., *Correlation of Double-Layer Capacitance with the Pore Structure of Sol-Gel Derived Carbon Xerogels*. Journal of The Electrochemical Society, 1999. **146**(10).
8. Moreno, A.H., et al., *Carbonisation of resorcinol-formaldehyde organic xerogels: Effect of temperature, particle size and heating rate on the porosity of carbon xerogels*. Journal of Analytical and Applied Pyrolysis, 2013. **100**: p. 111-116.
9. Carrott, P.J.M., F.L. Conceição, and M.M.L.R. Carrott, *Use of n-nonane pre-adsorption for the determination of micropore volume of activated carbon aerogels*. Carbon, 2007. **45**(6): p. 1310-1313.
10. Contreras, M.S., et al., *A comparison of physical activation of carbon xerogels with carbon dioxide with chemical activation using hydroxides*. Carbon, 2010. **48**(11): p. 3157-3168.

11. Virginia Hernández-Montoya, J.G.-S.a.J.I.B.-L., *Thermal Treatments and Activation Procedures Used in the Preparation of Activated Carbons*, in *Lignocellulosic Precursors Used in the Synthesis of Activated Carbon*. 2012, INTECH.
12. Zubizarreta, L., et al., *Tailoring the textural properties of activated carbon xerogels by chemical activation with KOH*. *Microporous and Mesoporous Materials*, 2008. **115**(3): p. 480-490.
13. Elkhataf, A.M. and S.A. Al-Muhtaseb, *Advances in tailoring resorcinol-formaldehyde organic and carbon gels*. *Adv Mater*, 2011. **23**(26): p. 2887-903.
14. Richard W. Pekala, P.H., Calif., *LOW DENSITY, RESORCINOL-FORMALDEHYDE AEROGELS*. 1988, The United States Department of Energy, Wash.
15. Rey-Raap, N., A. Arenillas, and J.A. Menéndez, *Carbon Gels and Their Applications: A Review of Patents*, in *Submicron Porous Materials*. 2017. p. 25-52.
16. Al-Muhtaseb, S.A. and J.A. Ritter, *Preparation and Properties of Resorcinol-Formaldehyde Organic and Carbon Gels*. *Advanced Materials*, 2003. **15**(2): p. 101-114.
17. Dochia, M., et al., *Cotton fibres*, in *Handbook of Natural Fibres*. 2012. p. 11-23.
18. Kim, B.K., et al., *Electrochemical Supercapacitors for Energy Storage and Conversion*, in *Handbook of Clean Energy Systems*. 2015. p. 1-25.
19. Pang, E.J.X., et al., *N-type thermoelectric recycled carbon fibre sheet with electrochemically deposited Bi₂Te₃*. *Journal of Solid State Chemistry*, 2012. **193**: p. 147-153.
20. Lin, C. and J.A. Ritter, *Carbonization and activation of sol-gel derived carbon xerogels*. *Carbon*, 2000. **38**(6): p. 849-861.
21. Job, N., et al., *Porous carbon xerogels with texture tailored by pH control during sol-gel process*. *Carbon*, 2004. **42**(3): p. 619-628.
22. Tsuchiya, T., et al., *Binderfree synthesis of high-surface-area carbon electrodes via CO₂ activation of resorcinol-formaldehyde carbon xerogel disks: Analysis of activation process*. *Carbon*, 2014. **76**: p. 240-249.
23. Frackowiak, E. and F. Beguin, *Carbon materials for the electrochemical storage of energy in capacitors*. *Carbon*, 2001. **39**(6): p. 937-950.

24. Zhai, Z., et al., *Carbon aerogels with modified pore structures as electrode materials for supercapacitors*. *Journal of Solid State Electrochemistry*, 2017. **21**(12): p. 3545-3555.
25. Mahani, A.A., S. Motahari, and V. Nayyeri, *Electromagnetic and microwave absorption characteristics of PMMA composites filled with a nanoporous resorcinol formaldehyde based carbon aerogel*. *RSC Advances*, 2018. **8**(20): p. 10855-10864.
26. Yang, I., et al., *Design of organic supercapacitors with high performances using pore size controlled active materials*. *Current Applied Physics*, 2019. **19**(2): p. 89-96.
27. Yun, S., et al., *Effects of carbonization temperature on structure and mechanical properties of monolithic C/SiO₂ aerogels based on ambient pressure dried superhydrophobic resorcinol-formaldehyde/SiO₂ aerogels*. *Journal of Porous Materials*, 2018. **25**(6): p. 1825-1830.
28. Liu, N., J. Shen, and D. Liu, *Activated high specific surface area carbon aerogels for EDLCs*. *Microporous and Mesoporous Materials*, 2013. **167**: p. 176-181.
29. Moon, C.-W., et al., *Effect of Activation Temperature on CO₂ Capture Behaviors of Resorcinol-based Carbon Aerogels*. *Bulletin of the Korean Chemical Society*, 2014. **35**(1): p. 57-61.
30. Cai, X., et al., *Preparation of Hierarchical Porous Carbon Aerogels by Microwave Assisted Sol-Gel Process for Supercapacitors*. *Polymers (Basel)*, 2019. **11**(3).
31. Ma, F., et al., *Sakura-based activated carbon preparation and its performance in supercapacitor applications*. *RSC Advances*, 2019. **9**(5): p. 2474-2483.
32. Wei, R., X. Dai, and F. Shi, *Enhanced CO₂ Adsorption on Nitrogen-Doped Carbon Materials by Salt and Base Co-Activation Method*. *Materials (Basel)*, 2019. **12**(8).
33. Yinghu Liu, J.S.X., Tao Zheng and J. R. Dahn, *Mechanism of lithium insertion in hard carbons prepared by pyrolysis of epoxy resins*. *Carbon*, 1996. **34**(2): p. 193-200.
34. Chavhan, M.P. and S. Ganguly, *Carbon cryogel from resorcinol formaldehyde: tuning of processing steps and activation for use in supercapacitor*. *Materials Technology*, 2017. **32**(12): p. 744-754.

35. Quach, N.K.N., et al., *Investigation of the Characteristic Properties of Glacial Acetic Acid-Catalyzed Carbon Xerogels and Their Electrochemical Performance for Use as Electrode Materials in Electrical Double-Layer Capacitors*. *Advances in Materials Science and Engineering*, 2017. **2017**: p. 1-9.
36. Osińska, M., et al., *The electrochemical performance of carbon xerogels with the addition of graphite intercalation compound*. *Applied Surface Science*, 2019. **481**: p. 545-553.
37. Yang, L., et al., *Effect of steam and CO₂ activation on characteristics and desulfurization performance of pyrolusite modified activated carbon*. *Adsorption*, 2016. **22**(8): p. 1099-1107.
38. Sirisomboonchai, S., et al., *Enhanced electrochemical performances with a copper/xylose-based carbon composite electrode*. *Applied Surface Science*, 2018. **436**: p. 639-645.
39. Jin-Young Jung, Y.-S.L., *Electrochemical properties of KOH-activated lyocell-based carbon fibers for EDLCs*. *Carbon Letters*, 2018. **27**: p. 112-116.
40. Oh, Y.J., et al., *Oxygen functional groups and electrochemical capacitive behavior of incompletely reduced graphene oxides as a thin-film electrode of supercapacitor*. *Electrochimica Acta*, 2014. **116**: p. 118-128.

APPENDICES

Appendix A: Calculations for carbon/carbon composite xerogels and content of cotton fibers

To synthesized carbon/carbon composite xerogels by using five main precursors, including Resorcinol, Formaldehyde, Sodium carbonate, Distilled water, and Cotton fibers. The amount of precursors for carbon/carbon composite xerogels synthesis

Table A-1 Synthesis conditions of carbon/carbon composite xerogels

Condition	Ratio	Unit
Resorcinol/Formaldehyde (R/F)	0.5	mol/mol
Resorcinol/Sodium carbonate (R/C)	200	mol/mol
Resorcinol/Distilled water (R/W)	0.250	g/cm ³

Table A-2 The amount of precursors for carbon/carbon composite xerogels synthesis

Materials	Molar Mass (g/mol)	Weight (g)
Resorcinol (R)	110.10	20.0000
Formaldehyde (F) 35-40% in methanol	30.03	29.4840
Sodium carbonate (C)	105.99	0.0963
DI Water (W)	18.02	61.4251

Table A-3 The amount of cotton fibers for carbon/carbon composite xerogels synthesis

Cotton fibers (wt.%)	CF/RF (g/g)	Weight of cotton fibers (g)
0	0	0
10	0.1	0.24
20	0.2	0.48
30	0.3	0.72
40	0.4	0.96

Appendix B: Calculations for the specific capacitance

B-1 Specific capacitance (C_c) from cyclic voltammogram

From
$$C_c = \frac{Q}{2 \times (V_2 - V_1) \times \mu \times m}$$

Where Q = the integrated area of the cyclic voltammogram

$V_2 - V_1$ = the potential window (V)

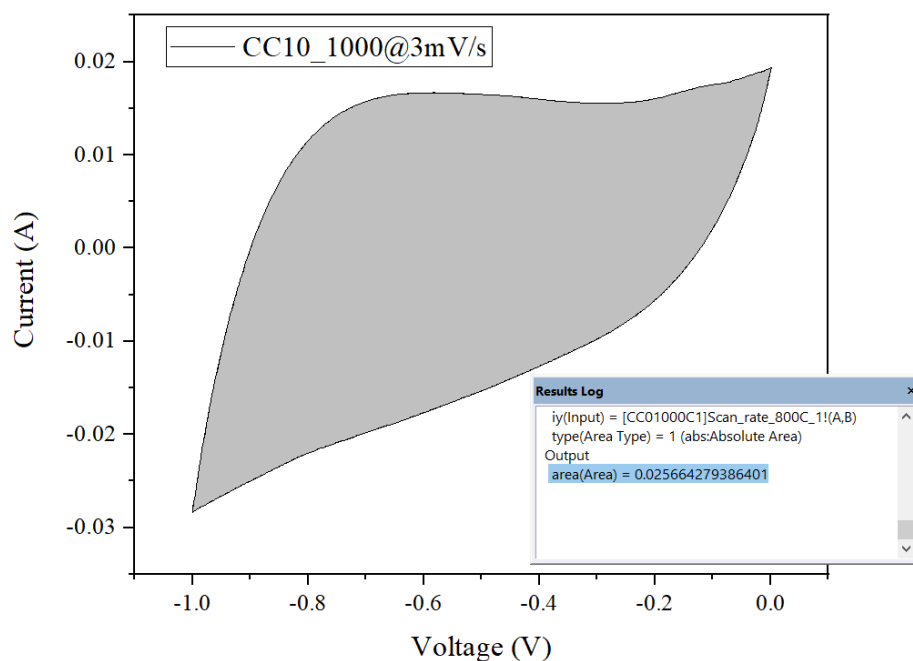
μ = the scan rate ($V s^{-1}$)

m = the mass of carbon/carbon composite xerogels on electrodes (g)

For example ; from cyclic voltammogram of CC10_1000C at scan rate $3 mV s^{-1}$

- The integrated area of the cyclic voltammogram from Origin Pro 2018 = 0.02566 AxV

So, $Q = 0.02566 \text{ AxV}$



- The potential window : $V_1 = -1 \text{ V}$ and $V_2 = 0 \text{ V}$
- The scan rate = 0.003 V s^{-1}

- The mass of carbon/carbon composite xerogels = 0.0233 g

$$\text{So, } C_C = \frac{0.02566 \text{ A}\cdot\text{V}}{2 \times (0 - (-1))\text{V} \times 0.003 \text{ V}\cdot\text{s}^{-1} \times 0.0233 \text{ g}}$$

$$C_C = \frac{183.55 \text{ A}\cdot\text{s}}{\text{V}\cdot\text{g}}$$

$$C_C = \frac{183.55 \text{ F}}{\text{g}}$$

- ∴ The specific capacitance (C_C) of CC10_1000C at scan rate $3 \text{ mV s}^{-1} = 183.55 \text{ F g}^{-1}$

B-2 Specific capacitance (C_D) from discharge curve

From
$$C_D = \frac{I \times (t_2 - t_1)}{2 \times (V_2 - V_1) \times m}$$

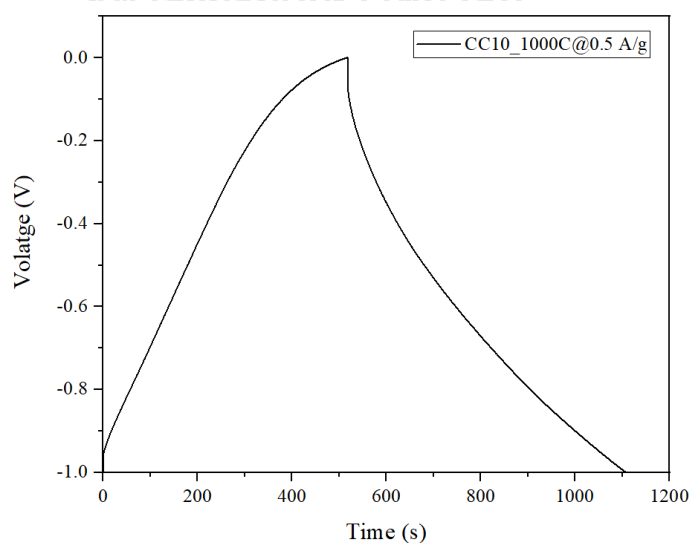
Where I = the discharge current (A)

$t_2 - t_1$ = the discharge time (s)

$V_2 - V_1$ = the potential window (V)

m = the mass of carbon/carbon composite xerogels on electrodes (g)

For example; from discharge curve of CC10_1000C at current density 0.5 A g^{-1}



- The discharge current = 0.011636 A

- The discharge time : $t_1 = 0$ s and $t_2 = 551$ s
- The potential window : $V_1 = -1.0028$ V and $V_2 = -0.1486$ V
- The mass of carbon/carbon composite xerogels = 0.0233 g

$$\text{So, } C_C = \frac{0.011636 \text{ A} \times (551-0)\text{s}}{2 \times ((-0.1486) - (-1.0028))\text{V} \times 0.0233 \text{ g}}$$

$$C_C = \frac{161.07 \text{ A}\cdot\text{s}}{\text{V}\cdot\text{g}}$$

$$C_C = \frac{161.07 \text{ F}}{\text{g}}$$

- ∴ The specific capacitance (C_D) of CC10_1000C at current density 0.5 A g^{-1} = 161 F g^{-1}



VITA

NAME Kasawan Sirichan

DATE OF BIRTH 19 February 1994

PLACE OF BIRTH Nakhonpathom

INSTITUTIONS ATTENDED Graduated high school from The Demonstration School of Nakhon Pathom Rajabhat University in 2012.
Graduated Bachelor's Degree faculty of Engineering and Industrial Technology in Petrochemicals and Polymeric Materials, Silpakorn University, Thailand in 2016.

HOME ADDRESS 189 Moo 10 Bangpla, Banglen, Nakhonpathom, 73130

PUBLICATION Sirichan, K., Bumroongsakulsawat, P., Assabumrungrat, S., and Kraiwattanawong, K. (2019, May 30) Effect of cotton fibers on carbon/carbon composite xerogels electrode for using in EDLCs. Proceedings of The 25th PPC Symposium on Petroleum, Petrochemicals, and Polymers, and The 10th Research Symposium on Petrochemical and Materials Technology, Bangkok, Thailand.